Pergamon

Geochimica et Cosmochimica Acta, Vol. 58, No. 10, pp. 2361–2386, 1994
Copyright © 1994 Elsevier Science Ltd
Printed in the USA. All rights reserved
0016-7037/94 $6.00 + .00

0016-7037(94)E0037-L

Chemical weathering rate laws and global geochemical cycles*

ANTONIO C. LASAGA, JOSEP M. SOLER, JIWCHAR GANOR,† TIMOTHY E. BURCH,‡ and KATHRYN L. NAGY§
Department of Geology and Geophysics, Yale University, New Haven, CT 06520-8109, USA

(*Received May* 3, 1993; *accepted in revised form January* 4, 1994)

Abstract—In this paper, we discuss the recent kinetic work on water-rock interactions. Standard activity-activity diagrams are reinterpreted, using a mass transfer kinetic model and recent data on the relative rates of mineral reactions. The development of a fully integrated rate law is discussed, with special attention to the important effects of deviation from equilibrium on the rates of mineral-water reactions. The combined effects of temperature, pH, ionic strength, and saturation conditions on the overall dissolution and precipitation rates of minerals must be properly described before any seriously quantitative model of coupled fluid flow and chemical reaction can be undertaken. A rate law that integrates these effects is proposed.

The functional dependence of the rate on ΔG_r, the free energy change for the mineral reaction, is discussed, based on recent experimental work. An important result is the presence of a surface transition in the reaction mechanism leading to a very strong nonlinear dependence of the dissolution rates on ΔG_r. The possible role of dislocation defects in this surface transition is discussed.

The relation of global weathering rates and geochemical cycles to the recent experimental and theoretical water-rock kinetic work is explored. The temperature effect on the silica content of streams is reevaluated. The variation of silica concentration with runoff in the rivers of the world is quantified, using a coupled fluid flow and reaction model and the full rate law developed for a proto-granite system by the kinetic experiments. Implications of the water-rock kinetic data for the current geochemical cycles models are discussed with especial emphasis on the link between physical weathering and chemical weathering.

INTRODUCTION

THERE IS MUCH CURRENT interest in understanding the factors that govern the chemical interactions between minerals and aqueous solutions. These chemical and physical processes, mediated by the surfaces of minerals, have profound effects on a wide variety of societal problems such as toxic wastes, radioactive wastes, acid rain, and acid mine drainage. Ultimately, the various chemical studies of water-rock interactions must be incorporated into high-level computer codes that couple the transport and the chemical reactions, thereby simulating (as realistically as possible) the scenarios taking place in nature. As in any model, many simplifying assumptions are invoked in any simulation. How well the simulation approaches reality will depend on the validity of these assumptions. While the transport codes have all been of necessity kinetic codes, the treatment of the chemistry involving minerals and solutions has quite often assumed that equilibrium is a valid approximation. As more field data accrues, it has become increasingly obvious that most earth surface processes are dominated by chemical kinetics. In turn, the basic processes that control the operations of various geochemical cycles cannot be understood without a proper kinetic framework.

Although it is widely recognized that disequilibrium processes may be controlling the occurrences of silicate and aluminosilicate mineral assemblages in low temperature environments, experimental data on reaction rates over the full range of solution saturation states are just now becoming available. Our understanding of the surface chemistry of silicate and aluminosilicate dissolution under conditions far from equilibrium is improving rapidly, due both to an increase in the abundance of experimental data and advances in surface analytical techniques. However, with the exception of silica (RIMSTIDT and BARNES, 1980; DOVE and CRERAR, 1990) and the recent data on kaolinite, gibbsite, and albite (NAGY et al., 1990, 1991; NAGY and LASAGA, 1992; BURCH et al., 1993), meager data have been available on the variation of dissolution rates of silicates and aluminosilicates over the range of undersaturation found in natural systems. Equally important, until recently, very little was known about the precipitation or growth kinetics of silicates and aluminosilicates in low temperature environments.

Full crystal growth and dissolution rate laws for minerals, which include the variation of the rates as equilibrium is approached, must be included in hydrodynamic models of fluid flow in porous or fractured media in order to accurately explain the observed mineral assemblages and textures in many water-rock systems. In such models, the rate laws which describe the reaction rates as a function of solution saturation state and temperature provide a feedback control on the fluid velocity through the porosity and permeability (STEEFEL and LASAGA, 1990, 1992; NAGY et al., 1990; STEEFEL and VAN CAPPELLEN, 1990).

There have been several approaches to incorporate the dissolution and precipitation of minerals in numerical models

* Paper presented at the "Symposium in Honor of Heinrich D. Holland" held May 8 and 9, 1992, in Reston, Virginia, USA.

† *Present address:* Ben Gurion University, Beer-Sheva 84105, Israel.

‡ *Present address:* Oak Ridge National Lab, MS6110, Oak Ridge, TN 37831, USA.

§ *Present address:* Exxon Production Research Co., P. O. Box 2189, Houston, TX 77252-2189, USA.

of fluid flow in water-rock systems. Earlier approaches assumed equilibrium for all minerals except a single slowly dissolving mineral, whose reaction determined the progress variable describing the evolution of the system (HELGESON, 1968, 1979). Later models (AAGAARD and HELGESON, 1982; LICHTNER, 1985, 1988) used kinetics for the dissolution rate of certain minerals, and then invoked the assumption of local or partial equilibrium (i.e., infinitely fast kinetics) for the precipitation of alteration minerals. In these models, the dissolution rate was taken to depend on pH and saturation state by use of transition state theory or TST-like equations. More recently, the models have used a kinetic treatment for both dissolution and precipitation (LASAGA, 1984; NAGY et al., 1990; STEEFEL and LASAGA, 1992, 1994) of all the minerals involved. For the latter approach, until now, the absence of precipitation rate data for aluminosilicates and silicates has required assuming that the principle of detailed balancing as well as the validity of TST-like equations for dissolution (LASAGA, 1981b, 1984; LAIDLER, 1987) apply to rate laws of overall reactions (NAGY et al., 1991; STEEFEL and VAN CAPPELLEN, 1990).

The data of NAGY et al. (1991) suggest that the principle of detailed balancing may not work for kaolinite dissolution and precipitation rates very near equilibrium (i.e., where the ΔG for the reaction is less than ± 1 kcal/mol). This is in contrast to the results of RIMSTIDT and BARNES (1980) on quartz dissolution and precipitation kinetics at temperatures up to 350°C and to the data on gibbsite (NAGY and LASAGA, 1992), which does appear to conform to the principle of detailed balancing near equilibrium. Note that the principle of detailed balancing is perfectly valid for elementary reactions. However, the applicability of it to surface reactions consisting of several possible mechanisms on either side of equilibrium is not at all as easy to prove. The kaolinite data is not conclusive, i.e., one can still defend detailed balancing within the error bars. Further work must be carried out to uncover the underlying physical chemistry governing the near-equilibrium region for many mineral reactions. In particular, the accuracy of the dissolution and precipitation rate measurements must be improved with new techniques so that competing theories can be better differentiated.

In addition to the exploration of the near-equilibrium region, all these experimental data have demonstrated that the precipitation rates of alteration minerals can be slow: minerals do not immediately crystallize out of supersaturated solutions, even in the presence of proper nucleation seeds. The relative rates of dissolution also vary widely, as evidenced in the field and the laboratory (see LASAGA, 1984). Table 1 gives an update of the earlier calculation of mean lifetimes of a 1 mm crystal (LASAGA, 1984), using data at 25°C and pH = 5, and assuming far from equilibrium conditions. Again, note that the rate of dissolution of alteration minerals (gibbsite and kaolinite) is comparable or slower than that of typical primary minerals, such as feldspars. This important result points out the problem with the use of the first and second approaches in modeling the evolution of a water-rock system, as discussed in the next section. Clearly the only satisfactory answer to the problem lies in accurate treatment of the kinetics of dissolution and precipitation. The important implications for global cycles will be discussed later in the paper.

MASS TRANSFER

The theory of mass transfer has been widely used in earth sciences and material sciences over the last decades. The application of mass transfer has focused mostly on interpreting the changes in mineralogy and/or chemical composition resulting from wallrock alteration, metasomatism, weathering, or similar reactions. The theory incorporates the simple idea of stoichiometry of a reaction into a treatment of slow (irreversible) reactions along with fast (equilibrium) reactions. It is in this domain where both equilibrium and kinetics are playing a role that mass transfer techniques become very useful.

Geochemists have traditionally used activity-activity diagrams (or stability diagrams) to represent the evolution of

TABLE 1. Mean Lifetime of a 1 mm Crystal at 25°C and Ph-5

Mineral	Log rate (mol/m²/s)	Mol. vol. (cm³/mol)	Lifetime (y)	References
Quartz	−13.39	22.688	34,000,000	Rimstidt and Barnes, 1980
Kaolinite	−13.28	99.52	6,000,000	Nagy et al., 1991 Carroll and Walther, 1988, 1990
Muscovite	−13.07	140.71	2,600,000	Lin and Clemency, 1981
Epidote	−12.61	139.2	923,000	Rose, 1991
Microcline	−12.50	108.741	921,000	Schweda, 1989
Prehnite	−12.41	140.33	579,000	Rose, 1991
Albite	−12.26	100.07	575,00	Burch et al., 1993 Knauss and Wolery, 1986 Chou and Wollast, 1985
Sanidine	−12.00	109.008	291,000	Schweda, 1989
Gibbsite	−11.45	31.956	276,000	Nagy and Lasaga, 1992 Mogollón et al., 1994
Enstatite	−10.00	31.276	10,100	Schott et al., 1989
Diopside	−10.15	66.09	6,800	Schott et al., 1989
Forsterite	−9.5	43.79	2,300	Blum and Lasaga, 1988
Nepheline	−8.55	55.16	211	Tole et al.,1986
Anorthite	−8.55	100.79	112	Fleer, 1982
Wollastonite	−8.00	39.93	79	Rimstidt and Dove, 1986

the chemistry of the solutions in weathering or alteration processes (GARRELS and CHRIST, 1965; DREVER, 1988). The construction of these diagrams (see Fig. 1) assume equilibrium between any coexisting mineral phases. Therefore, depending on the solution composition, only one mineral can be present within a particular stability field, and several minerals can only coexist along the boundaries of these stability fields. The interpretation of data plotted on activity-activity diagrams relies heavily on the assumption that local or partial equilibrium is quickly established between the alteration minerals shown and the adjacent solutions.

Because the use of activity-activity diagrams is so prevalent, it is important to test the validity of the kinetic assumptions implicit in their construction. It should be emphasized, however, that even if kinetics is playing a major role in the reactions of fluids and minerals, the activity-activity diagrams themselves provide a very useful depiction of the chemical composition of solutions. Nonetheless, the common usage of the activity-activity diagrams to interpret the fluid composition data would be definitely inappropriate in a kinetically controlled natural system. Because kinetic data are now available for dissolution and precipitation of feldspar, kaolinite, and gibbsite (BURCH et al., 1993; NAGY et al., 1991; NAGY and LASAGA, 1992), the chemical weathering of a granite presents an ideal test case. The evolution of a solution interacting with a granite under the usual assumptions of local equilibrium can be represented using the stability diagrams in Fig. 1. In the example, the initial pH is taken as 4.4, $T = 25°C$, and the solution has initially no Si, Al, or K. Such a solution could represent a typical acidic meteoric solution. The assumptions in the calculation were that the dissolution of K-feldspar is slow and irreversible. However, upon saturation of the solution with any of the alteration products, equilibrium between the solution and the mineral is instantaneously achieved. The path in Fig. 1 shows the usual sequence of alteration products. Initially, gibbsite precipitates; at a later time, supersaturation with respect to kaolinite causes the precipitation of kaolinite and the subsequent dissolution of gibbsite. This segment of the evolution is shown by the vertical line tracking the boundary between gibbsite and kaolinite in the activity-activity diagram. Finally, all the gibbsite dissolves, and the solution composition moves into the kaolinite stability field. Ultimately, the system approaches equilibrium with the feldspar. The mineral sequences show this sequence in detail (Fig. 1b). Note that the appearance of kaolinite is marked by the initial decrease in gibbsite abundance in Fig. 1b. The horizontal axis in Fig. 1b marks the progress variable, ξ, for the dissolution of feldspar (i.e., how many moles dissolved)

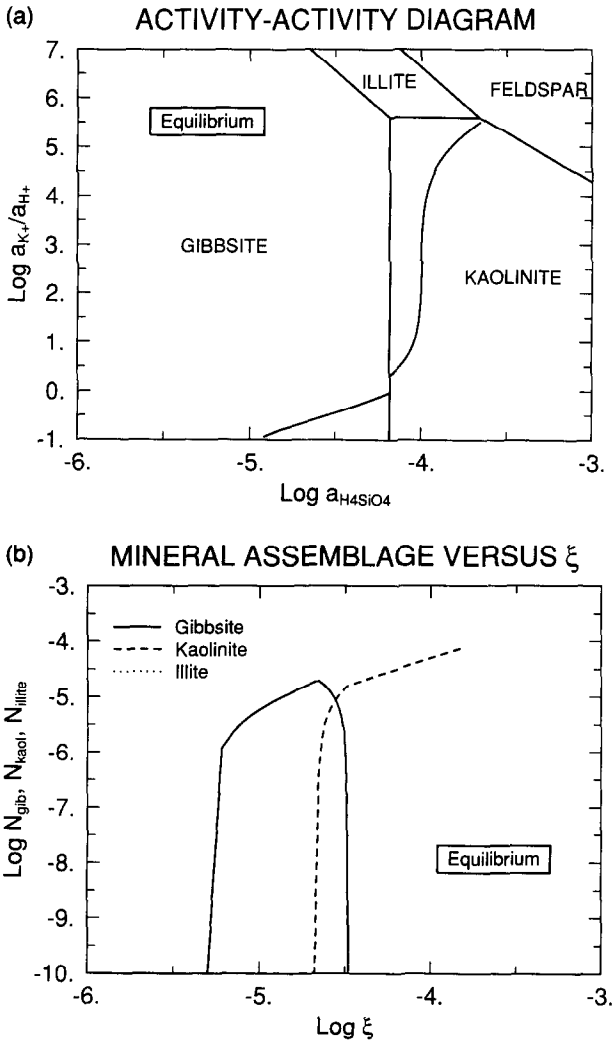

FIG. 1. (a) Activity-activity diagram showing the chemical composition path of a solution in equilibrium with a dissolving feldspar. The solution starts with a composition close to rainwater. (b) Evolution of the mineral assemblage as a function of the progress variable of the system (taken as the dissolution of the feldspar—Eqn. 1). The moles of the different minerals are given, using a logarithmic scale.

$$KAlSi_3O_8 + 4H^+ + 4H_2O \rightarrow K^+ + Al^{3+} + 3H_4SiO_4. \quad (1)$$

Our purpose is to understand the role of kinetics in modifying the typical assumptions inherent in the previous calculation. Therefore, these reaction path calculations need to be extended to include a general treatment of dissolution and precipitation kinetics for all the minerals involved. Based on the progress variable for the feldspar reaction, ξ, the rate of dissolution of feldspar is clearly

$$\frac{dn_{K-\text{feldspar}}}{dt} = -\frac{d\xi}{dt}, \quad (2)$$

or

$$\frac{dn_{K-\text{feldspar}}}{d\xi} = -1. \quad (3)$$

Typically, n and ξ in the last two equations are normalized, so that their units are in moles per unit volume of rock or moles per unit volume of solution. In our calculations, we used units of moles per Kg solution. The kinetic treatment needs to consider the dissolution and precipitation rate of gibbsite:

$$Al^{3+} + 3H_2O \rightleftharpoons \underset{\text{gibbsite}}{Al(OH)_3} + 3H^+, \quad (4)$$

and kaolinite:

$$2Al^{3+} + 2H_4SiO_4 + H_2O \rightleftharpoons \underset{\text{kaolinite}}{Al_2Si_2O_5(OH)_4} + 6H^+. \quad (5)$$

with a similar reaction for illite (muscovite). Because all the mineral reactions will be treated as slow, only the speciation in solution is treated as an equilibrium process in the new mass transfer calculations. The kinetic mass transfer calculations still require the rates of mineral reactions to be cast in terms of one progress variable, the feldspar dissolution progress variable, ξ. Therefore, if R_i refers to the net rate of precipitation or dissolution of a particular mineral i (in moles per unit time per unit volume of rock), the calculations use the relation

$$\frac{dn_{\text{gibbsite}}}{d\xi} = \frac{R_{\text{gibb}}}{R_{\text{feld}}}. \quad (6)$$

To present the consequences of kinetics as succinctly as possible, the true kinetic rate laws (see later section) have been simplified to those that are common near equilibrium. Therefore, the rate laws have been assumed to follow a linear dependence on free energy:

$$R_i = k_i \frac{\Delta G_i}{RT}, \quad (7)$$

where ΔG_i refers to the net free energy change of reactions 1, 4, and 5, and k_i is a rate constant. Note that Eqn. 7 is used for both the precipitation and the dissolution rate. This equation is consistent with the principle of detailed balancing applied to the overall reaction. Note also that k_i is not an intrinsic rate constant, but incorporates any surface area factors into its magnitude (LASAGA, 1984). If ΔG is too large, the recent research has shown that Eqn. 7 is not valid; however, we will overlook that problem in this section, because the aim is to show the effect of relative kinetics on the validity of activity-activity diagrams.

The behavior of the system is now determined by the relative values of the rate constants in Eqn. 7, as well as the values of ΔG_i. For example, the equilibrium calculation carried out before is equivalent to assuming that the k_i/k_{feldspar} ratio for gibbsite, kaolinite, and illite is sizable. What sizable means will be made precise in what follows.

While in actuality the relative rates of the minerals are quite different, the role of kinetics in the model can be illustrated with a series of calculations which vary the ratio k_i/k_{feldspar}, but keeps the ratio constant for all alteration minerals. The common value of k_i/k_{feldspar} was allowed to range from 0.1 to 1000. The results are shown in Figs. 2–6. It is instructive to actually see the approach to equilibrium as the rate constants are increased. The results for $k_i/k_{\text{feld}} = 1000$ are shown in Fig. 2. In this case, the full kinetic treatment leads to a mass transfer calculation that is very similar to the equilibrium case (i.e., only feldspar dissolution is kinetically sluggish). Both the solution composition (Fig. 2a) and the mineralogy (Fig. 2b) conform quite closely to the equilibrium case (Fig. 1). Therefore, sizable has now been redefined as 1000 times faster than the rates of the primary minerals.

Reducing the ratio of k_i/k_{feldspar} to 100 already leads to some deviations from the classical equilibrium results (Fig. 3). In particular, the solution composition does not follow the boundaries of mineral pairs (e.g., gibbsite-kaolinite). Therefore, some gibbsite is present within the stability field of kaolinite. The mineralogy plot (Fig. 3b) shows that now there is a small region where both gibbsite and kaolinite increase contemporaneously, and thus the region containing both gibbsite and kaolinite increases over that in the equilibrium case. As the ratio k_i/k_{feldspar} decreases further to 10 or 1, the most evident changes in the evolution are shown by the mineralogy plots (Figs. 4b and 5b). In the case that k_i/k_{feldspar} is 10, the region of metastable coexistence of gibbsite and kaolinite grows significantly. The mineralogical evolution for the case that $k_i/k_{\text{feldspar}} = 1$ shows that illite (muscovite) is now appearing in the alteration even though the solution

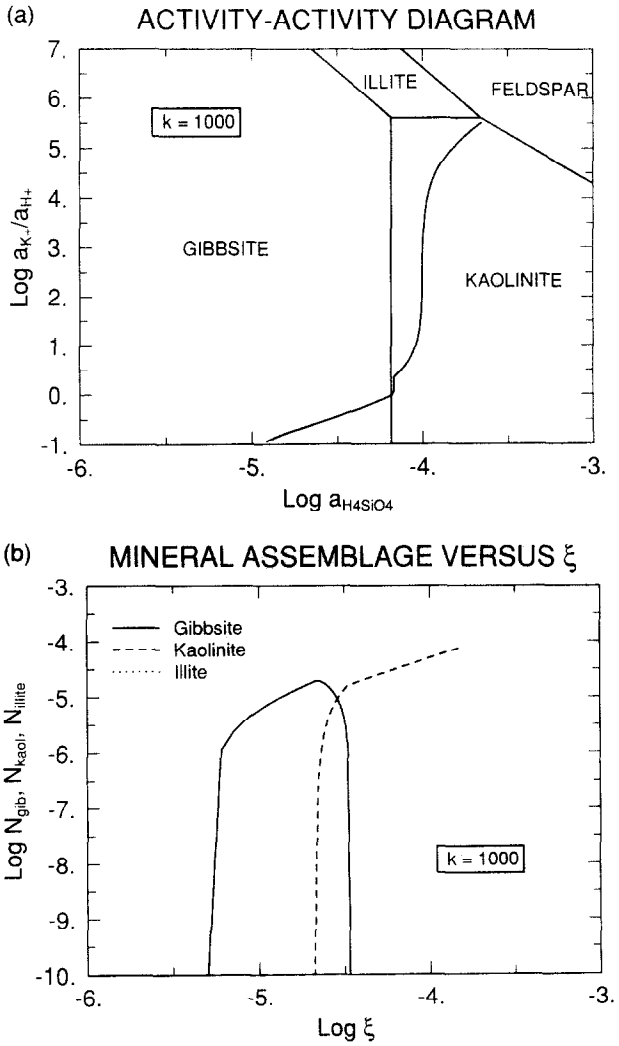

FIG. 2. (a) Activity-activity diagram showing the chemical composition path of a solution with the same initial composition as in Fig. 1 but now governed by the kinetics of both dissolving and precipitating minerals. In this calculation, the kinetic rate constants (e.g., k_i in Eqn. 5) of all the alteration minerals are taken to be 1000 times bigger than the rate constant for the dissolving feldspar. Note the close similarity to Fig. 1a. (b) The evolution of the mineral assemblage as a function of the progress variable of the system (which is still taken to be the number of moles of feldspar dissolved). Again, note the similarity to Fig. 1b.

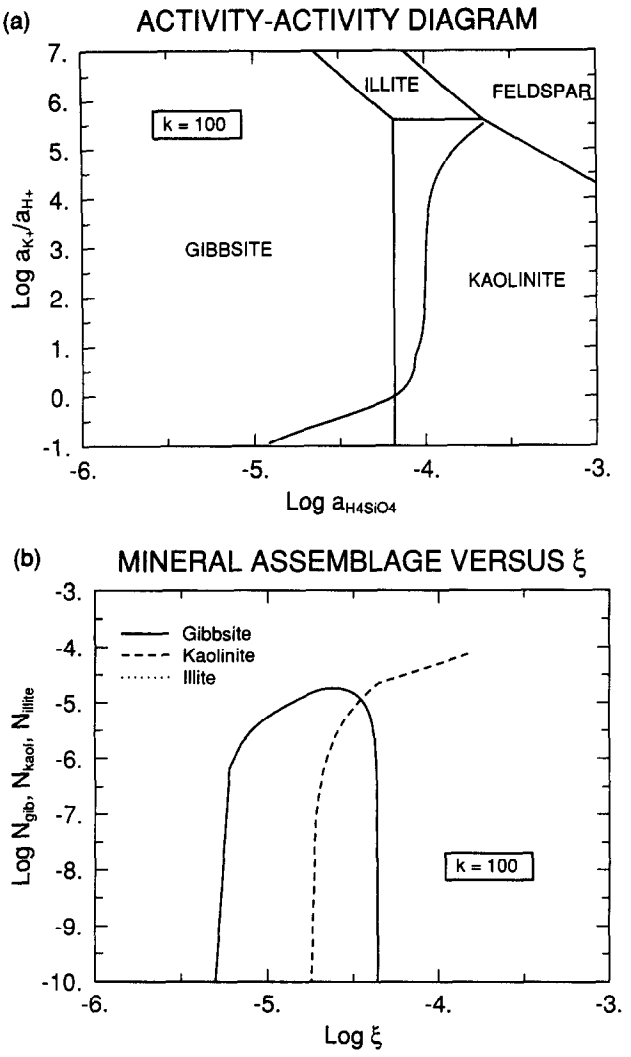

FIG. 3. (a) Same as Fig. 2a, but now the rate constants of the alteration products are 100 times bigger than that of feldspar. Note that now the solution composition does not follow the kaolinite-gibbsite boundary. (b) Same as Fig. 2b, but with the rate constants for the alteration products 100 times bigger than that for feldspar. Note that there is now a region where both gibbsite and kaolinite are precipitating.

composition, as plotted on the activity-activity plot (Fig. 5a), never reaches the muscovite stability field. However, in this case, muscovite appears only as gibbsite disappears. By the time that $k_i/k_{feldspar}$ is 0.1 (Fig. 6), the three alteration minerals coexist over an extended region. This coexistence, of course, reflects the slow precipitation rates of the alteration minerals.

It is interesting to note that the marked variations in the mineralogical evolution are not apparent from looking at the evolution of the solution composition on the activity-activity diagrams (e.g., compare Figs. 3a and 6a). Therefore, an important result is the higher sensitivity of the mineral sequences to the kinetics than the solution composition. This result is important because often, it is only the mineralogy that remains for us to analyze in the field, not the actual solutions that led to the chemical changes.

The recent experimental data (such as summarized in Table 1) can now be viewed from the point of view of the results obtained in this section. As shown in Table 1 and discussed in the next section, recent kinetic data predicts a $k_i/k_{feldspar}$ ratio of 10 for gibbsite and 0.1 for kaolinite, assuming equal surface areas and far from equilibrium conditions. Obviously, these new data and the results of this section cast doubt on the unqualified validity of the activity-activity plot interpretation. Of course, if the reactive surface areas of the alteration minerals were extremely large (e.g., 100 times feldspar for gibbsite and 10,000 times feldspar for kaolinite), the k_i would be adequately high and the equilibrium model would be tenable. On the other hand, smaller surface areas would lead to even further deviations from the equilibrium model than shown in this section. Therefore, the treatment of chemical weathering must take into account the rate laws of alteration minerals as well as those of the primary minerals in the rock.

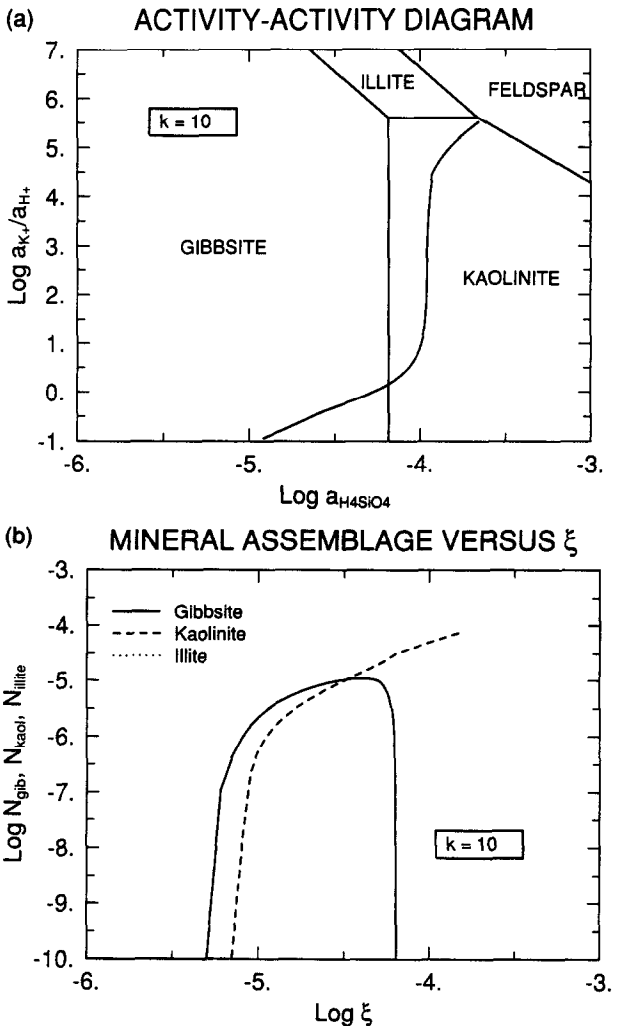

FIG. 4. (a) Same as Fig. 2a, but now the rate constants of the alteration products are ten times bigger than that of feldspar. The solution pathway does not deviate that much from that of Fig. 3b in the rest of the series. (b) Same as Fig. 2b, but with the rate constants for the alteration minerals ten times bigger than that for feldspar. There is now extensive coexistence of gibbsite and kaolinite.

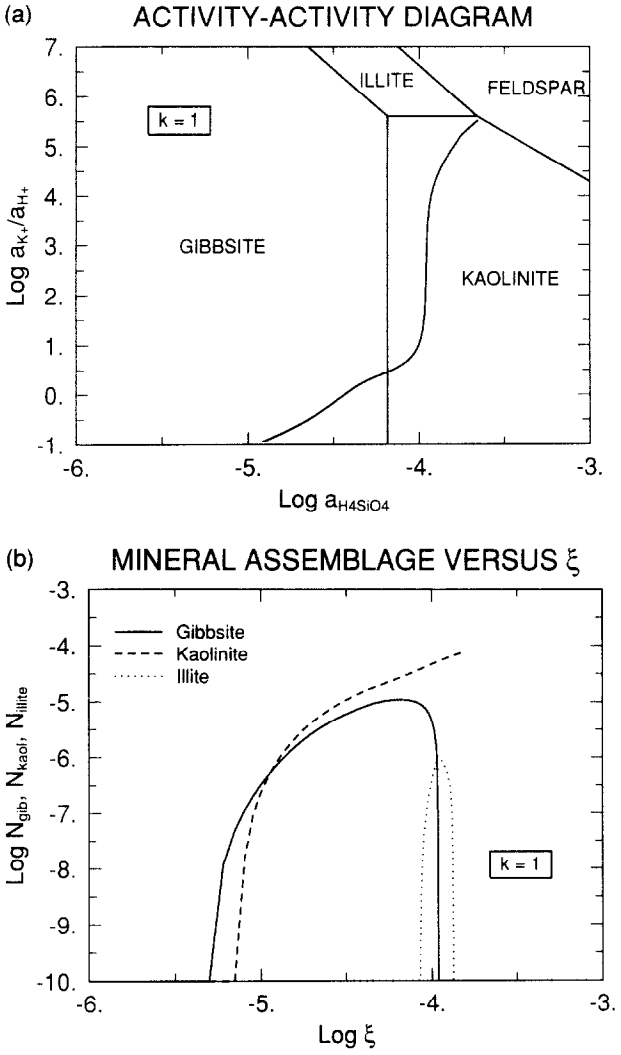

FIG. 5. (a) Same as Fig. 2a, but now the rate constants of the alteration products are the same as that of feldspar. The one new difference is the inflection of the curve as it crosses the gibbsite-kaolinite boundary. (b) Same as Fig. 2b but with the rate constants for the alteration minerals the same as that of feldspar. Even though the stability field of illite is never reached (in the activity-activity diagram), the system is now precipitating and then dissolving illite. Note that the illite comes and goes, while the kaolinite still increases.

As the next section emphasizes, however, the rate laws are more complex than Eqn. 7. Therefore, the ratio k_i/k_{feldspar} is likely to vary by more than an order of magnitude during the chemical evolution of a particular solution in contact with a granite or an arkose. Nonetheless, the major result from this section is that, based on data such as given in Table 1, the analysis of geochemical field observations using activity-activity plots requires a careful evaluation of kinetic mineral-fluid reaction data. Therefore, the next step that extends the simple calculations of this section is a careful appraisal of our current knowledge about the rate laws of mineral-fluid interactions.

SURFACE CHEMISTRY AND RATE LAWS

The importance of understanding the chemical processes at mineral surfaces has been well appreciated by numerous workers in recent years. In particular, the role that these processes play in determining the overall kinetic rate of dissolution/precipitation or adsorption/desorption reactions has been analyzed. Two factors that have received a lot of attention have been temperature and solution pH. Certainly, these two factors exert a pivotal role in the overall rate law for dissolution or precipitation of minerals. However, any hope of modeling the behavior of the solid crust in the presence of water requires that the possibility of achieving equilibrium be included in the model. This inclusion cannot be carried out if the rate law for the various mineral-water reactions does not incorporate the critical change of the rate with deviation from equilibrium. As will be discussed further below, one of the most interesting discoveries of our recent work has been the nontrivial variation of the rates with deviation from equilibrium. Of course, this result has a number of important implications for our modeling of chemical weathering

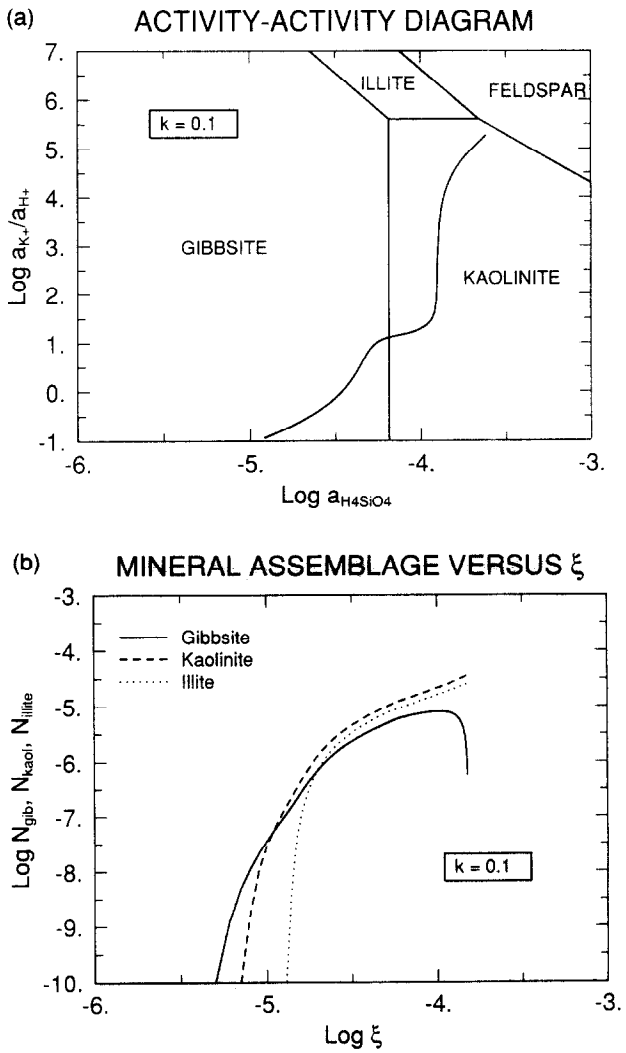

FIG. 6. (a) Same as Fig. 2a, but now the rate constants of the alteration products are 0.1 times smaller than that of feldspar. Note the extensive inflection of the solution path. (b) Same as Fig. 2b but with the rate constants for the alteration minerals 0.1 times smaller than that of feldspar. There is now extensive coexistence of gibbsite, kaolinite, and illite.

and geochemical cycles, implications that will be explored later in the paper.

A general form of the net rate law for heterogeneous mineral surface reactions can be written as

$$\text{Rate} = k_0 A_{\min} e^{-E_a/RT} a_{H^+}^{n_{H^+}} \prod_i a_i^{n_i} f(\Delta G_r), \qquad (8)$$

where $A_{\min}$ is the reactive surface area of the mineral, and E_a is the activation energy of the overall reaction. The much studied pH dependence of the dissolution/precipitation reactions has been written explicitly in Eqn. 8. The terms involving the activities of other species in solution, a_i, incorporate other possible catalytic or inhibitory effects on the overall rate. Such catalysis or inhibition is kinetically quite distinct from the final term, $f(\Delta G_r)$, which accounts for the important variation of the rate with the deviation from equilibrium ($\Delta G_r = 0$). The one sure constraint comes from thermodynamics; in fact, within the kinetic framework being developed here, all of thermodynamics is embedded in the statement

$$f(0) = 0. \qquad (9)$$

This relation simply states that the net rate of an overall reaction must be zero at equilibrium (i.e., $\Delta G_r = 0$), and guarantees that the kinetics will be fully compatible with thermodynamics. If, furthermore, the principle of detailed balancing is applicable to the overall reaction, then the derivative of f at equilibrium, $f'(0)$, is well-defined (i.e., has the same value as equilibrium, is approached from undersaturation ($\Delta G_r \leq 0$) or supersaturation ($\Delta G_r \geq 0$)). The existence of $f'(0)$ renders valid the application of the theory of irreversible thermodynamics, which requires linear relations between fluxes and forces (DEGROOT and MAZUR, 1962; FISHER and LASAGA, 1981). However, in the field of crystal growth, the theory of irreversible thermodynamics may not be always applicable, even very close to equilibrium between a mineral and the composition of a solution, especially when nonequilibrium defects in the mineral play a major role in the kinetics (LASAGA, 1981a). The shape of the function f will be discussed further below. Aside from this singularly important point (i.e., $f(0)$), the function is not constrained other than requiring that precipitation take place (a positive value in our convention) for supersaturated solutions (ΔG_r positive), and that dissolution takes place (ΔG_r negative) for undersaturated solutions. To be sure, certain simple growth theories such as transition state theory or the Burton-Cabrera-Frank (BCF) theory (BURTON et al., 1951) predict a form for the function f (linear and quadratic respectively for sufficiently small ΔG_r), but the actual form of f requires deliberate experimental work. As the detailed form of the $f(\Delta G_r)$ function is obtained for different minerals, molecular kinetic theories (e.g., at the level of elementary reactions on mineral surfaces similar to the BCF treatment) will be needed to explain the results (LASAGA, 1990). It is the term $f(\Delta G_r)$ that embodies the ability of the rate law to adjust the rate to the important deviations from equilibrium.

The functional dependence of the rate on the overall ΔG_r is essential to any attempts to apply the experimental kinetic data to natural processes. Our ignorance of the role of this function in the interpretation of mineral dissolution kinetic data is a major flaw in current kinetic work. For example, differentiating catalytic or inhibitory effects (e.g., Al effects on feldspar dissolution) from the effects of $f(\Delta G_r)$ are very important in further interpretation of the kinetics.

The importance of understanding the behavior of kinetic systems in relation to the deviation from equilibrium may affect even calculations of activation energies. For example, if a series of experiments at different temperatures are carried out and the ionic strength and pH are fixed, Eqn. 8 leads to

$$\ln \text{Rate} = \ln(\text{constant}) - E_a/RT + \ln f(\Delta G_r). \qquad (10)$$

If $f(\Delta G_r)$ varied in the different experiments as the temperature varied (a factor often ignored) then the calculated activation energy will pick up a spurious term. This term may be several kcal/mol in magnitude. This problem would be minimal only in the far-from-equilibrium region. Under sufficiently dilute solutions (very negative ΔG_r), the dissolution rate would become independent of ΔG_r and f would take on a constant value. Unfortunately the definition of far-from-equilibrium can only be known after experiments on the particular minerals have been carried out. For example, the albite data (BURCH et al., 1993) have shown that the ΔG_r needed to be far-from-equilibrium exceeded -10 kcal/mol for the reaction written as in Eqn. 1. Therefore, some of the experiments by previous workers may not have been in the far-from-equilibrium region (e.g., the kinetic data of KNAUSS and WOLERY, 1986, on albite dissolution which agrees very nicely with the data of BURCH et al., 1993, as discussed in the latter paper). Furthermore, the degree of deviation from equilibrium in mineral-water experiments is a strong function of the pH of the experiments. For example, the recent experiments by CASEY et al. (1993) on tephroite show the approach to equilibrium of the solutions as the pH increased in the dissolution experiments. Only if the shape of the $f(\Delta G_r)$ function is known, can other effects such as catalysis, inhibition, or the effect of temperature be properly handled.

Some of the recent work (KLINE and FOGLER, 1981a,b; FURRER and STUMM, 1986; BLUM and LASAGA, 1988, 1991; CASEY and SPOSITO, 1992; BRADY and WALTHER, 1992) has pointed out the importance of writing the kinetic rate laws using the concentration (or activity) of adsorbed reactants on the mineral surface. Following their lead, it would be better to write our general rate law as

$$\text{Rate} = k_0 A_{\min} e^{-E_a/RT} X_{H^+,\text{ads}}^{n_{H^+,\text{ads}}} \prod_i X_{i,\text{ads}}^{n_i} f(\Delta G_r), \qquad (11)$$

where for most reactions, equilibrium can be assumed between the mole fraction of adsorbed species on the mineral surface, $X_{i,\text{ads}}$, and the solution composition. For any given mineral, then, $X_{i,\text{ads}}$ will be a function of pressure, temperature, and the solution composition.

Finally, the reaction mechanism may change under varying temperature, pressure, or solution compositions (e.g., acid or basic conditions). Therefore, the last equation can be generalized further to

$$\text{Rate} = A_{\min} \sum_j k_{0,j} e^{-E_{a,j}/RT} X_{H^+,\text{ads}}^{n_{H^+,\text{ads},j}} \times X_{OH^-,\text{ads}}^{n_{OH^-,\text{ads},j}} \prod_i X_{i,\text{ads}}^{n_{i,j}} f_j(\Delta G_r), \qquad (12)$$

where the exponents, the activation energies, and even the $f(\Delta G_r)$ function can change. While Eqn. 12 may strike one as being unwieldy, in practice the experimental work has shown that only two terms are usually needed to describe the kinetic data. Thus, in many cases one would have

$$\text{Rate} = A_{\min} k_{0,\text{acid}} e^{-E_{a,\text{acid}}/RT} X_{H^+,\text{ads}}^{n_{H^+,\text{ads}}} f_{\text{acid}}(\Delta G_r) + A_{\min} k_{0,\text{basic}} e^{-E_{a,\text{basic}}/RT} X_{OH^-,\text{ads}}^{n_{OH^-,\text{ads}}} f_{\text{basic}}(\Delta G_r), \quad (13)$$

which can probably be further simplified to

$$\text{Rate} = A_{\min}[(k_{0,\text{acid}} e^{-E_{a,\text{acid}}/RT} X_{H^+,\text{ads}}^{n_{H^+,\text{ads}}} + k_{0,\text{basic}} e^{-E_{a,\text{basic}}/RT} X_{OH^-,\text{ads}}^{n_{OH^-,\text{ads}}}] f(\Delta G_r), \quad (14)$$

with a common $f(\Delta G_r)$ function. Nonetheless, the main point being made here is that the verity of these rate laws must be checked after proper experimental work has been carried out, including the critical variation of the rate with ΔG_r, as well as the precipitation rates. For many minerals, the data have yet to be collected.

The Function $f(\Delta G_r)$

The form of the ΔG_r function, $f(\Delta G_r)$, depends on the reaction mechanism(s) operating during both dissolution and precipitation. One of the goals of our experimental work is to identify major theoretical concepts needed to predict $f(\Delta G_r)$. The function $f(\Delta G_r)$ is readily obtained when the overall mechanism consists of an elementary reaction (LASAGA, 1981a; NAGY et al., 1991). In this case, $f(\Delta G_r)$ can be derived from transition state theory (TST), and is given by (LASAGA, 1981b, 1984; AAGAARD and HELGESON, 1982):

$$f(\Delta G_r) = -(1 - \exp(\Delta G_r/RT)), \quad (15)$$

where ΔG_r is the Gibbs Free Energy of the overall reaction (kcal/mol), R is the gas constant, and T is the temperature (K). Note that this equation does satisfy $f(0) = 0$. If Eqn. 15 is substituted into Eqn. 8, it follows that at constant temperature and surface area, the dissolution rate will be independent of ΔG_r, far from equilibrium (large negative ΔG_r), and controlled by the activity of components i (e.g., H^+ or OH^- or ionic strength) in solution. This region in Rate-ΔG_r space where the rate is constant is termed the dissolution plateau (NAGY et al., 1991). According to Eqn. 15, the dissolution plateau would be reached if $\Delta G_r \ll -RT$. Note that near equilibrium, Eqn. 15 yields a linear dependence on ΔG_r, and the full Eqn. 8 reduces to an expression similar to that used earlier in Eqn. 7.

Near equilibrium, Eqn. 15 predicts that the rate will be a linear function of ΔG_r for both dissolution and precipitation rates

$$\text{Rate} = k_{\text{eff}} \Delta G_r, \quad (16)$$

where k_{eff} incorporates all the other terms (in Eqn. 8 or 11). Therefore, if the overall reaction is truly described by the same elementary reaction, then there is no kink in the rate law on either side of equilibrium. This behavior is supported by our data on gibbsite (NAGY and LASAGA, 1992) and possibly by the data on albite (BURCH et al., 1993; T. BURCH, pers. commun.). However, as mentioned earlier, the kaolinite data, although in agreement with the TST formulation for the rate law given the uncertainty in the data, may also be interpreted as suggesting the presence of a kink (NAGY et al., 1991).

For overall reactions, however, the function $f(\Delta G_r)$ is difficult to predict a priori (NAGY et al., 1991; NAGY and LASAGA, 1992). Often, workers have generalized Eqns. 14 and 15 to

$$f(\Delta G_r) = -[1 - \exp((n\Delta G_r)/RT)], \quad (17)$$

where now the constant n is not necessarily equal to 1 (AAGAARD and HELGESON, 1982). Equation 17 is valid only when certain conditions are met; and these conditions may not apply to all cases. Equation 17 is not valid if nonequilibrium defects such as dislocations are controlling the reaction kinetics. One case where Eqn. 17 is valid is that in which a complex reaction sequence of elementary reactions has all elementary reactions occurring near equilibrium, except for a single elementary reaction involved in a slow rate-determining step. In this case, Eqn. 17 is valid with $n = 1$. A second, more common case is that in which a steady-state is established in the entire sequence of elementary steps (i.e., the stoichiometry of the overall reaction is maintained during the kinetic process). In this case, Eqn. 17 is valid for small values of $\Delta G_r/RT$, and is approximately correct for larger values (see NAGY et al., 1991). Note that in the second case, $n \neq 1$.

The BCF theory makes another prediction for the form of the $f(\Delta G_r)$ function. In its simplest case, the theory derives for the case of precipitation

$$f(\Delta G_r) = (\exp(\Delta G_r/RT) - 1)^2. \quad (18)$$

Note that the BCF theory will never reduce to a linear ΔG_r dependence, no matter how close the system approaches to equilibrium, i.e., it is an intrinsically nonlinear theory (and as such not consistent with the linear theory of irreversible thermodynamics because of the role of extended defects; see LASAGA, 1981b). Near equilibrium, the BCF rate law reduces to

$$\text{Rate} = k\Delta G_r^2. \quad (19)$$

The BCF theory originated as a growth theory, although it can be extended to the case of mineral dissolution (BLUM and LASAGA, 1987). The basic premise requires that dislocations crop out on the exposed mineral surface, and thereby provide a series of atomic steps for crystal growth through the ensuing formation of an Archimedean spiral (the steps being separated by the distance travelled by the spiral in one swing). Both the rate of attachment of atoms to the steps via surface diffusion and the spacing of the steps in the spiral are proportional to ΔG_r, which results in a nonlinear dependence of the net growth rate on ΔG_r. A variety of simple inorganic systems obey Eqn. 19 (at least for precipitation); see NIELSEN (1986) for a recent summary.

Over the range of saturation states expected in nature, the $f(\Delta G_r)$ function exhibits even more complex behavior than the simpler cases discussed in this section, at least for the dissolution rates. The study of precipitation rates has been limited by the requirement of having only one phase precipitating at any one time. Recent work with simultaneous pre-

cipitation of gibbsite and kaolinite (NAGY and LASAGA, 1993), has shown that it is possible to extend the earlier work to a broader range of positive ΔG_r, by using experiments which have solutions that are supersaturated with respect to more than one mineral.

Deviation from Equilibrium, $f(\Delta G_r)$ and the New Role of Defects

Recent work has produced the experimental $f(\Delta G_r)$ functions for dissolution of kaolinite, gibbsite, and albite that are given in Figs. 7, 8, and 9 (NAGY et al., 1991; NAGY and LASAGA, 1992; BURCH, 1993). The $f(\Delta G_r)$ functions are obviously quite nontrivial. Furthest from equilibrium, rates are independent of ΔG_r. This region is the dissolution plateau where most previous experimental work has been conducted. In this region, free energy terms can be neglected in the dissolution reaction rate law, Eqn. 8. Closer to equilibrium, rates increase rather sharply with decreasing ΔG_r. Near equilibrium, rates are dependent on ΔG_r, but to a much lesser extent, approaching direct proportionality to ΔG_r as given by Eqn. 8 or 9.

The term far from equilibrium must be used with caution. The experimental data for albite (Fig. 9) demonstrate that the dissolution rate is independent of ΔG_r only for solutions with $\Delta G_r \leq -9$ kcal · mol^{-1} undersaturated (using Eqn. 1), corresponding to $\Delta G_r/RT \leq -13$. The gibbsite dissolution rate (Fig. 7) is independent of solution saturation state only for solutions with $\Delta G_r \leq -0.5$ kcal · mol^{-1} undersaturated, or $\Delta G_r/RT \leq -0.7$ (using Eqn. 3 to calculate ΔG_r). Future work needs to delineate further this important transition for other minerals.

The most impressive feature of these nontrivial f functions is the dramatic increase in the rate as a certain critical undersaturation is reached. This discovery of a mechanistic transition in the rate law has been linked to the role of surface defects. NAGY and LASAGA (1992) and BURCH et al. (1993) have shown that the abrupt change in dissolution rate for gibbsite and albite is related to the role of dislocations in

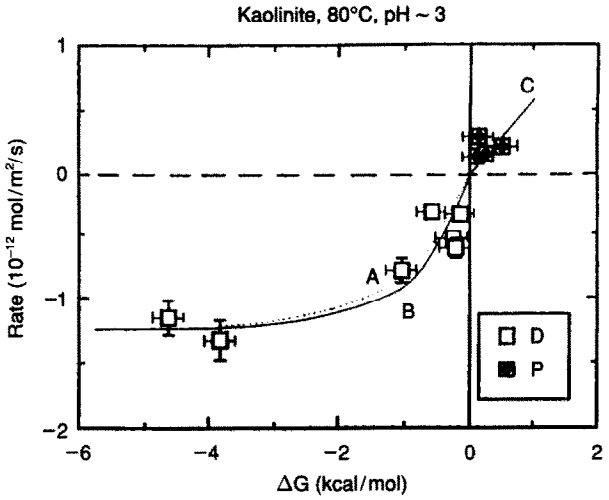

FIG. 8. Kaolinite precipitation (positive) and dissolution (negative) rates as a function of $\Delta G_r/RT$. ΔG_r is the free energy change of the reaction $Al_2Si_2O_5(OH)_4 + 6\ H^+ \rightarrow 2\ Al^{3+} + 2\ H_4SiO_4 + H_2O$. Experimental data at 80°C and pH 3 from NAGY et al. (1991).

mineral dissolution kinetics. LASAGA (1983) had shown how a critical undersaturation is necessary to etch dislocation cores at the surface of a mineral. LASAGA and BLUM (1986) showed that the density of etch pits on a mineral surface is a function of the crystallographic orientation of the dislocation (Burgers vector) and type (edge vs. screw). On this basis, they proposed that examination of natural mineral grains would be highly useful as a record of paleofluid saturation state. BRANTLEY et al. (1986) provided experimental evidence supporting the correlation of visible etch pits on quartz with the degree of undersaturation in hydrothermal fluids. BLUM and LASAGA (1987) studied etch pit formation using Monte Carlo computer simulations, which included surface diffusion, and further showed that the shapes of etch pits as a function of solution undersaturation were in close agreement with the predictions of the earlier theory. BLUM and LASAGA (1987)

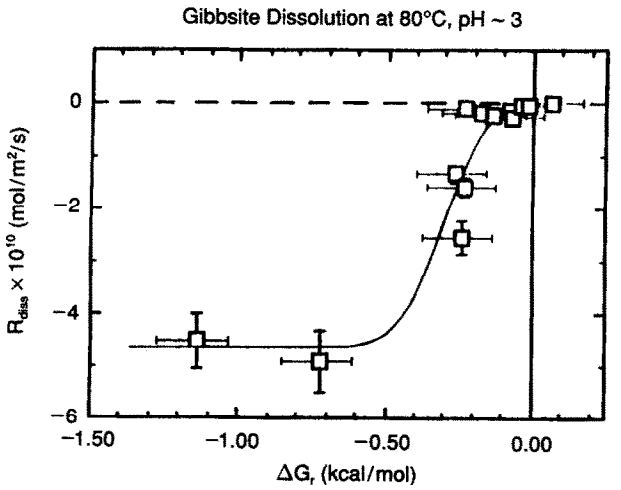

FIG. 7. Gibbsite dissolution rates vs. ΔG_r for the reaction $Al(OH)_3$ (gibbsite) + $3H^+ \rightarrow Al^{3+} + 3\ H_2O$. Experimental data at 80°C and pH 3 from NAGY and LASAGA (1992).

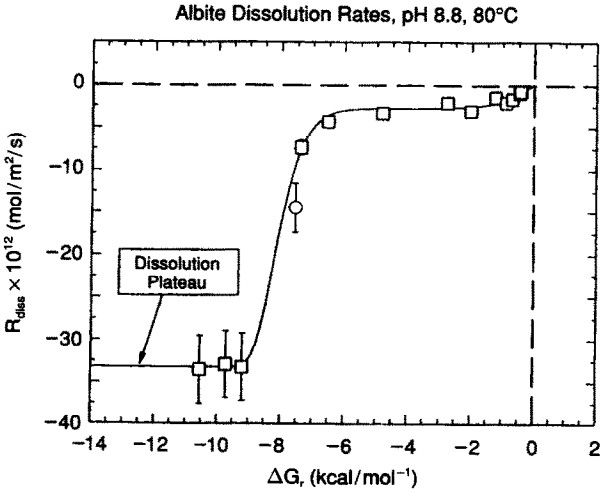

FIG. 9. Albite dissolution rates vs. ΔG_r for the reaction $NaAlSi_3O_8 + 8\ H_2O \rightarrow Na^+ + Al(OH)_4^- + 3\ H_4SiO_4$. Experimental data at 80°C and pH 8.8 from BURCH et al. (1993).

showed that the form of dissolution and crystal growth rate laws could be related to the defect or dislocation density of a mineral. In particular, BLUM and LASAGA (1987) obtained that dissolution rates should be positively correlated with dislocation density but only at very high dislocation densities. Experimental work on a variety of minerals with varying dislocation densities (e.g. chalcopyrite; MURR and HISKEY, 1981), rutile (CASEY et al., 1988), feldspar (HOLDREN et al., 1988; MURPHY, 1989a,b), quartz (BLUM et al., 1990), and calcite (SCHOTT et al., 1989)) has supported their theoretical prediction. At typical dislocation densities ranging from 10^6 cm^{-2} to 10^{11} cm^{-2}, dissolution rates in the dissolution plateau vary by at most a factor of three. Both the Monte Carlo work of BLUM and LASAGA (1987) and all of these experimental studies had in common that only the far from equilibrium dissolution rate (i.e., rate in the dissolution plateau) was being considered. BLUM et al. (1990) proposed that dislocation density variations may have a much larger effect on bulk dissolution rates near equilibrium, at saturation states where macroscopic etch pits should not form, i.e., above the critical undersaturation, ΔG_r, for etch pit formation. The importance of the near-equilibrium region was also stressed by BRANTLEY et al. (1986) and SCHOTT et al. (1989).

Our experimental findings shed new light on the whole topic of the role of defects in water-rock kinetics. Based on (1) observations of the reacted surfaces and (2) theoretical considerations, the mechanistic transition in the rates can be strongly related to the opening of dislocations in these minerals. The critical ΔG at which a dislocation core can open up to form an etch pit for the various minerals is (LASAGA and BLUM, 1986)

$$\Delta G_{crit} = -\frac{2\pi^2\sigma^2 K}{\mu b^2}\bar{V}, \qquad (20)$$

where σ is the surface free energy, K is a constant dependent on type of dislocation ($K = 1$ for a screw dislocation and $K = 1 - \nu$, where ν is the Poisson ratio, for an edge dislocation), $\bar{V}$ is the molar volume of the mineral, μ is the bulk shear modulus (dyne/cm^2), and b is the magnitude of the Burgers vector (Å). Calculations using available data for gibbsite and albite (see Table 2) lend credibility to the supposition that ΔG_{crit} correctly predicts the dramatic change in dissolution mechanism observed in our experimental results. The hypothesis has been further supported by SEM analysis of reactant and product mineral surfaces in both cases (NAGY and LASAGA, 1992; BURCH et al., 1993).

While clearly, more work is needed to understand this important phenomenon (the surface transition), there is little doubt that a major change in the kinetics is taking place. If the surface transition is also present in other minerals, then one can use relevant data for the variables in Eqn. 13 to calculate the region of rapid change in the dissolution rate. For example, the data in LASAGA and BLUM (1986) can be used to predict the ΔG_{crit} for forsterite and enstatite, which is important for modeling the weathering of basalt or mafic rocks. ΔG_{crit} for forsterite would range from -0.5 to -2.9 kcal/mol and for enstatite from -0.5 to -1.8 kcal/mol. NAGY and LASAGA (1992) calculated a ΔG_{crit} for calcite, and suggested that the experimental data of BERNER and MORSE (1974) may in part be explained by this mechanism. HUANG (1993) has shown that the ΔG_{crit} for kaolinite may occur at about -0.2 kcal/mol, using experimental dissolution rates determined as a function of ΔG_r at 200 and 275°C. Assuming that rate laws for other minerals are also a function of ΔG_{crit} (only for lack of new experimental data), the variations in dissolution rates of forsterite and enstatite, for example, could be estimated as a function of ΔG_r as long as the rate in the dissolution plateau were known. In fact, the experimental data on albite and gibbsite dissolution rates yield very similar plots when plotted vs. $\Delta G_r/\Delta G_{crit}$.

TABLE 2. Critical undersaturation ΔG_r^{crit} to etch dislocation in gibbsite and albite.

Gibbsite[1]			
		ΔG_r^{crit} (kcal · mol^{-1})	
$\vec{b}$	b (cm · 10^{-8})	Screw	Edge
[001]	9.72	−0.380	
[010]	5.07		−0.175
Albite[2]			
		ΔG_r^{crit} (kcal mol^{-1})	
$\vec{b}$	b (cm · 10^{-8})	Screw	Edge
[101]	10.842	−3.328	−2.425
[100]	8.142	−5.901	−4.299
[001]	7.159	−7.632	−5.562

[1] Calculation assumes: σ = 483 erg/cm^2; $\bar{V}$ = 31.956 cm^3 mol^{-1} ρ = 2.44 g cm^{-3}; $\mu = 3.09 \times 10^{11}$ dyne/cm^2; ν = 0.3.
[2] Calculation assumes: σ = 500 erg/cm^2; $\bar{V}$ = 100.07 cm^3 mol^{-1} ρ = 2.620 g cm^{-3}; $\mu = 7.211 \times 10^3$ cal/cm^{-3}; ν = 0.271.

Note that it is likely that other effects may also play a role in the rate laws of other minerals. The important phenomenon, which is likely to be quite general, is the ability of surfaces to undergo dramatic structural responses, as the ΔG_r of the solution changes and reaches some threshold. For example, some complex cases may exhibit several phase transitions or steps in the rate vs. ΔG_r curves. Nonetheless, this type of behavior is fundamentally very different from the linear or near-linear rate laws predicted by transition state theory. As discussed below, the changes in the rates will be relevant to the overall transport of silica in rivers and streams as well as to the workings of the C geochemical cycle.

Activation Energies

The temperature dependence of the dissolution and precipitation rates is significant and is typically expressed using the Arrhenius law

$$k = Ae^{-E_{app}/RT}, \qquad (21)$$

where A is the pre-exponential factor and E_{app} is the apparent activation energy of the mineral-fluid reaction. Because several elementary reactions may be involved in determining the size of E_{app}, we have used the label apparent to distinguish it from the classical activation energy of an elementary re-

action, such as treated by chemical collision theory (scattering theory) or by transition state theory. Because the temperature affects the exponential in Eqn. 21, temperature effects are clearly very important in affecting the rates. In addition, the effects of temperature can provide unique insights into the reaction mechanisms (LASAGA and GIBBS, 1990).

Recent studies have obtained apparent activation energies of mineral-solution reactions (see Table 3). The general range of apparent activation energies from recent work still leads to an average around 15 kcal/mol as suggested by LASAGA (1984). Note that an E_{app} = 15 kcal/mol will produce an increase of the rate by one order of magnitude between 0 and 25°C and another increase of an order of magnitude between 25 and 55°C.

As the rate law in Eqn. 11 implies, the temperature dependence of the overall dissolution and precipitation mineral reactions may be more complex than the temperature dependence of an elementary reaction. Hence, we have used the term apparent activation energy, E_{app}, in Eqn. 21. In fact, some of the recent work (CARROLL and WALTHER, 1990; CASEY and SPOSITO, 1992; BRADY and WALTHER, 1992) has focused on the variation of the apparent activation energy with pH. Because adsorption phenomena play such an important role in the dissolution/precipitation reactions, it follows that the apparent activation energy would pick up a contribution from the enthalpy of the adsorption process as discussed in LASAGA (1981b). Using Eqn. 11, one can write

$$-\frac{\partial \ln \text{Rate}}{\partial(1/T)} = \frac{E_{app}}{R} = \frac{E_a}{R} - n_{H+,ads}\frac{\partial \ln X_{H+,ads}}{\partial(1/T)} - n_{i,ads}\frac{\partial \ln X_{i,ads}}{\partial(1/T)} - \frac{\partial \ln f(\Delta G_r)}{\partial(1/T)}. \quad (22)$$

TABLE 3. Activation energies of minerals.

Mineral	E_a (Kcal/mol)	pH	References
Albite	13	Neutr	Knauss and Wolery, 1986
Albite	7.7	Basic	Knauss and Wolery, 1986
Albite	28	<3	Knauss and Wolery, 1986
Albite	17.1	1.4	Rose, 1991
Andalusite	11.5	1	Carroll, 1989
Andalusite	5.8	2	Carroll, 1989
Andalusite	1.8	3	Carrol, 1989
Epidote	19.8	1.4	Rose, 1991
Kaolinite	16.0	1	Carroll and Walther, 1990
Kaolinite	13.3	2	Carroll and Walther, 1990
Kaolinite	10.3	3	Carroll and Walther, 1990
Kaolinite	7.7	4	Carroll and Walther, 1990
Kaolinite	2.3	6	Carroll and Walther, 1990
Microcline	12.5	3	Schweda, 1989
Prehnite	20.7	6.5	Rose, 1991
Prehnite	18.1	1.4	Rose, 1991
Quartz	17.0	7	Dove and Crerar, 1990
Sanidine	12.9	3	Schweda, 1989
Tephroite	12.9	2.5	Casey et al., 1993
Tephroite	6.3	3.5	Casey et al., 1993
Tephroite	5.7	4.2	Casey et al., 1993
Tephroite	1.1	5.1	Casey et al., 1993
Wollastonite	18.9	3–8	Rimstidt and Dove, 1986

CASEY and SPOSITO (1992) have justified the pH dependence of the apparent activation energy from the second term in Eqn. 22. They obtain a pH dependence from the influence of the surface charge on the equilibrium constant for adsorption of hydrogen ions. Because the overall rate depends on a variety of factors (e.g., Eqn. 11 or 12), it is not surprising that the apparent activation energy could vary with pH. However, further experiments must be carried out to ascertain whether the variation is only due to pH or to the other factors in Eqn. 11. Ultimately, what must be done is to eliminate the adsorption terms and extract the actual activation energy, E_a, in Eqn. 11. Thus, if adsorption isotherms are known as a function of temperature, $X_{ads}(T)$, one can obtain E_a from the slope of a plot of ln k vs. $1/T$, where k is defined as

$$k \equiv \frac{\text{Rate}(T)}{X_{ads}(T)^n}, \quad (23)$$

as long as the rate is obtained in the dissolution plateau (i.e., the last term in Eqn. 17 is not important). Note that even here, one is making the assumption that the exponent n in the rate expression is not a function of temperature, i.e., the mechanism of the reaction does not change.

Compensation Law

One method of estimating activation energies from limited data is to show the existence of a compensation law (LASAGA, 1981b). The compensation law relates the pre-exponential in an Arrhenius equation to the activation energy for a wide variety of experimental measurements, i.e., if

$$k = Ae^{-E/RT},$$

then the compensation law states that

$$\ln A = a + bE. \quad (24)$$

Much has been written on the compensation law (LASAGA, 1981c) and it has been applied to an amazingly varied set of physical and chemical phenomena. If Eqn. 24 were to be valid, a measurement of a dissolution or precipitation rate at some temperature could be used to extract an activation energy (because we have two relations in two unknowns, A and E). An interesting result from the recent experimental data is the existence of a compensation law in the mineral-fluid rate constants. CASEY et al. (1993) exhibit such a compensation law for the pH dependence of the apparent activation energies of tephroite, andalusite, and kaolinite (the latter two using the data of CARROLL, 1989). These plots can be extended further. When combined with new available data on prehnite, epidote, wollastonite, quartz, and albite (see figure caption for references), the result is shown in Fig. 10a. The data obey the equation

$$\ln A = -16.77 + 0.720E_{app}, \quad (25)$$

where A is in units of moles/cm^2/s and the apparent activation energy, E_{app}, is in kcal/mol. If one just takes the data for tephroite, kaolinite, and andalusite used by CASEY and SPOSITO (1992), the line (Fig. 10b) would be

$$\ln A = -18.38 + 0.968E_{app}. \quad (26)$$

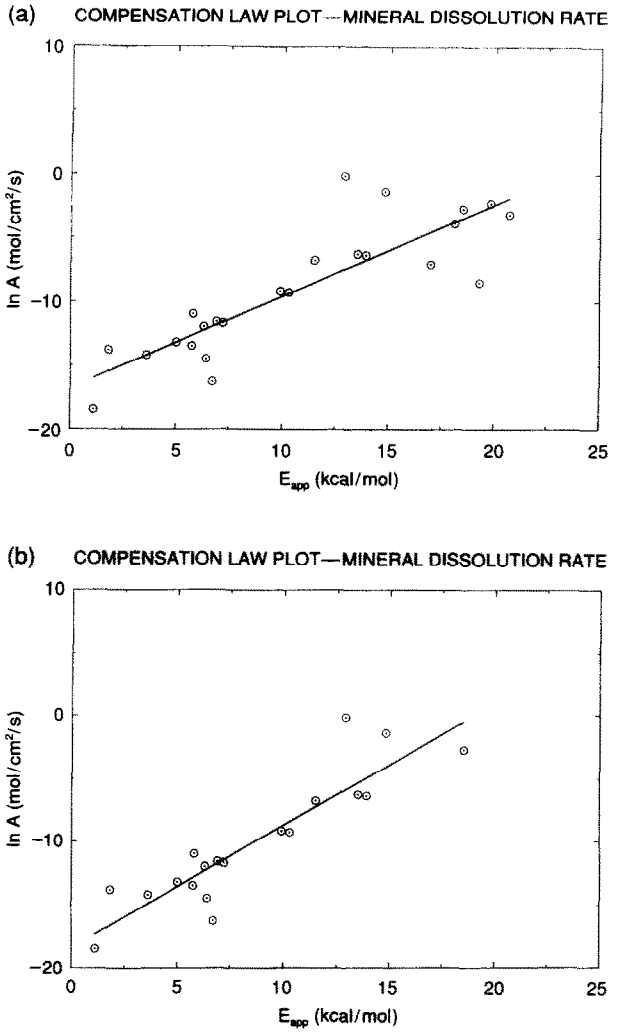

FIG. 10. (a) Compensation law plot for mineral dissolution rates. Data sources are tephroite data from CASEY et al. (1993); kaolinite and andalusite data from CARROLL (1989) (as quoted in CASEY and SPOSITO, 1992); prehnite, albite, and epidote data from ROSE (1991); wollastonite data from RIMSTIDT and DOVE (1986); quartz data from DOVE and CRERAR (1990). (b) Compensation law plot for the minerals tephroite, kaolinite, and andalusite. Data come from the same sources as in (a).

One of the interesting predictions of a compensation law is the existence of a temperature where all the rate constants are the same (LASAGA, 1981a). This universal temperature is given by

$$T_{\text{universal}} = \frac{1}{Rb}, \tag{27}$$

where R is the gas constant. The compensation laws in Eqns. 25 and 26 yield universal temperatures of 425 and 236°C, respectively. It is interesting that if one just takes the tephroite compensation law (from the data of CASEY et al., 1993), then the universal temperature comes out around 45°C. In this case, this temperature reflects the similarity in the experimental rates obtained at the various pH conditions studied (data in pH range 2.5 to 5.15 was used in estimating $T_{\text{universal}}$). Obviously, in the case of the data in Fig. 10a, the universal temperature is quite high. Nonetheless, because the universal temperature is higher than 25°C, the compensation law generally concludes that the mineral-water reaction rates among different minerals become more similar as the temperature is raised. Of course, as the temperatures reach 200°C, new reaction mechanisms may be operative, so that one may not be allowed to extrapolate the low temperature kinetic data up to the universal temperature itself.

While it is clear that there is a strong relation between ln A and E_{app}, it is not clear how far one can take the compensation law between the various minerals. Certainly the variations from a straight line in Fig. 10a are nontrivial. Perhaps, as the true activation energies are ascertained (see above), the compensation relations may be better extracted and, more importantly, more meaningfully interpreted, using atomic theory.

Activation Energy and Global Cycles

The activation energy is important in determining the temperature dependence of chemical weathering in nature. Such dependence has been used in modeling geochemical cycles (BERNER et al., 1983 (BLAG)). In the BLAG treatment, one of the key negative feedbacks on increases of CO_2 in the atmosphere is the increase in the weathering rate of silicates as a result of the increased global temperature. The formulation of BLAG used an effective activation energy of 8.1 kcal/mol (based on river data), which is lower than the mean value as pointed out by BRADY (1991). The data on silica concentration of rivers as a function of mean temperature from MEYBECK (1980) yield apparent activation energies of 3.8 kcal/mol (for volcanic rocks) and 9.1 kcal/mol (for nonvolcanic rocks). It is interesting to compare these activation energies to the Q_{10} factor used by soil scientists (BOHN et al., 1979). The Q_{10} factor is the increase in the rate of a soil reaction upon a 10°C increase in temperature. Typical Q_{10} values lie between 2 and 4. These Q_{10} values translate into activation energies between 11 and 22 kcal/mol, values strikingly similar to the mineral rate activation energy range.

A higher activation energy for chemical weathering will lead to a stronger negative feedback between CO_2 and weathering rate. In turn, such a stronger feedback will lead to more subdued variations of CO_2 with time, as will be discussed later in the paper.

An interesting point should be raised regarding the Arrhenius law. In most geochemical cycle models, the rates are linked to the mean value of the temperature, whether the local temperature, the regional temperature (MEYBECK, 1980), or the global temperature (BERNER et al., 1983). Given a yearly variation in temperature, however, the average that needs to be input into the rate equation is different than the average temperature, and the difference is a function of the amplitude of the variation. To see this, let us assume that T follows the yearly variation

$$T = \bar{T} + \Delta T \sin(2\pi t), \tag{28}$$

where $\bar{T}$ is the average temperature, ΔT is the amplitude of the variation, and t is time in years. The average rate constant under these conditions is given by

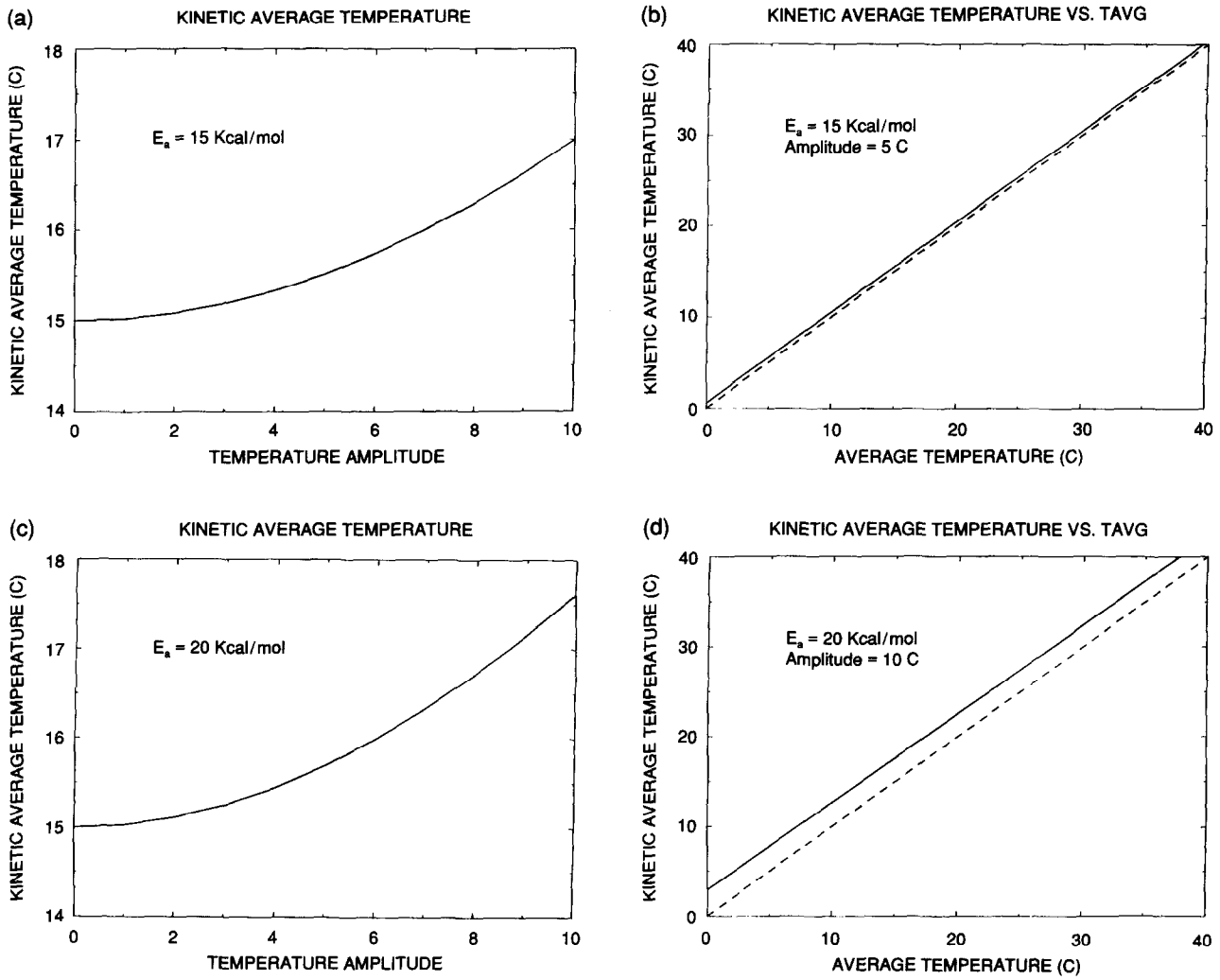

FIG. 11. (a) The kinetic average temperature, $\bar{T}'$, defined in eqn. 24 of text as a function of the amplitude of the variation in the seasonal temperature, ΔT (in Eqn. 22). The seasonal average temperature, $\bar{T}$ (Eqn. 22), is in all cases 15°C. The apparent activation energy of the reaction is assumed to be the canonical mean value for mineral dissolution reactions, 15 kcal/mol (LASAGA, 1984). (b) Variation of the kinetic average temperature, $\bar{T}'$ with the average temperature, $\bar{T}$, for a constant amplitude of ΔT = 5°C. (c) Same as (a) but now employing a higher apparent activation energy of 20 kcal/mol. (d) Same as (b), but now using 20 kcal/mol for the apparent activation energy and 10°C for the seasonal amplitude.

$$\bar{k} = A \int_0^1 e^{-\frac{Ea}{r}\frac{1}{T+\Delta T\sin(2\pi t)}} dt. \qquad (29)$$

If we set $\bar{k}$ to

$$\bar{k} = Ae^{-E_a/R\bar{T}'}, \qquad (30)$$

$\bar{T}$ and $\bar{T}'$ will not be the same. Figure 11a shows the nontrivial variation of the kinetic mean temperature, $\bar{T}'$, with the amplitude of the yearly variation. Figure 11 assumes that E_a is 15 kcal/mol and that the mean temperature, $\bar{T}$, is 15°C. Figure 11b shows the variation in $\bar{T}'$ with $\bar{T}$ at a constant small amplitude of 5°C. Figure 11c and d give the same results for an activation energy of 20 kcal/mol and an amplitude of 10°C. Note that the important change is to always increase the kinetic average because increases in temperatures speed up reactions more than equal decreases in temperatures slow them down. The result of the nonlinear relation between temperatures and rates is that the mean of the function in Eqn. 30 is not equal to the function evaluated at the mean temperature.

Given the important difference between $\bar{T}$ and $\bar{T}'$, it is interesting to reanalyze the MEYBECK (1980) data. A linear fit to the raw data yields an activation energy of 9.1 kcal/mol as mentioned earlier. However, the amplitude of the yearly temperature fluctuation is much bigger for northern latitudes (lower mean temperatures) than for rivers closer to the equator. As a simple correction the amplitude, ΔT, was taken to vary with mean temperature (and hence latitude) as

$$\Delta T = 15.87 - 0.533\bar{T}, \qquad (31)$$

based on surface temperature profiles for current earth (using the data from Global Ecosystems Database; KINEMAN, 1992) and where $\bar{T}$ is in Celcius. (Do not confuse the 15.87 with $\bar{T}$.) Note that much more sophisticated functions than Eqn.

31 could be used, and also that soil temperatures and seasonal fluctuations will be a function of depth; however, as a first approximation to (as usual) a much more complicated problem, Eqn. 31 should suffice to establish the main point of this section. With this relation, the earlier data of MEYBECK (1980) for nonvolcanics was corrected (i.e., for a given $\bar{T}$, the amplitude was obtained from Eqn. 31 and this ΔT used along with E_a = 15 kcal/mol to obtain $\bar{T}'$). A plot of the corrected concentration versus $\bar{T}'$ is shown in Fig. 12. Now the activation energy increases to values between 11 and 14 kcal/mol, much more in line with the bulk of experimental water-rock kinetic data. Such a nontrivial shift underscores the need to differentiate between Eqns. 22 and 23 in evaluating field studies.

Effects of Ionic Strength, pH, and Solution Composition on the Rates

Other solution properties that have been shown to affect the dissolution and precipitation rates are pH, solution ionic strength, and the concentration of individual species. The effect of pH on the rates has been studied extensively (BLOOM and ERICH, 1987; BLUM and LASAGA, 1988, 1991; FURRER and STUMM, 1986; BRADY and WALTHER, 1989; CARROLL and WALTHER, 1988, 1990; CHOU and WOLLAST, 1984; HELGESON et al., 1984; KNAUSS and WOLERY, 1986, 1988, 1989; STUMM and WIELAND, 1990; TOLE et al., 1986; WIELAND et al., 1988; BRADY, 1992; SCHWEDA, 1989; ROSE, 1991; CASEY et al. 1993; XIE and WALTHER, 1992; WOGELIUS and WALTHER, 1991). Generally speaking, the rates obey the rate law

$$\text{Rate} = k a_{\text{H}}^{n}, \qquad (32)$$

with n having values somewhere between −1 and 1. The pH dependence can be derived from the adsorption isotherm of H^+ or OH^- onto the mineral surfaces (FURRER and STUMM, 1986; BLUM and LASAGA, 1988; CARROLL-WEBB and WALTHER, 1988). In the near-neutral region (e.g., pH = 4–8) the pH dependence has usually been found to be slight, especially for aluminosilicates. This slight dependence of the rate of pH in the near-neutral region is similar to the slight effect of pH on the solubility of these minerals in the same region. These effects reflect the speciation of Al (and silica in some cases) both in solution and on the surface of the minerals (STUMM and WOLLAST, 1990).

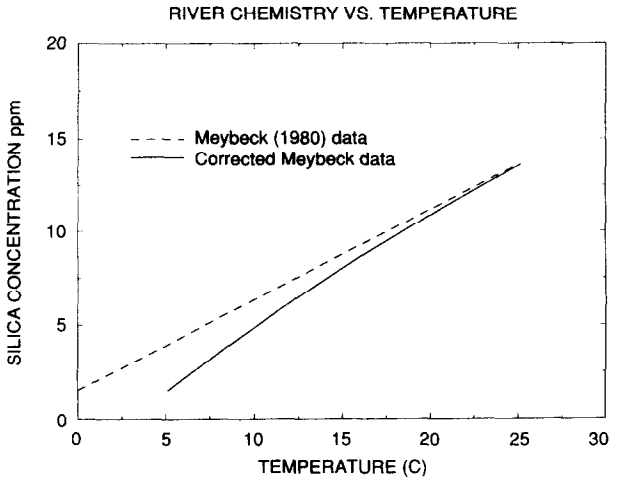

FIG. 12. Plot of the MEYBECK (1980) river silica concentration data as a function of mean annual temperature, $\bar{T}$ (——). The slope of the curve yields an activation energy of 9 kcal/mol. Correction of the mean annual temperature, $\bar{T}$, to the mean kinetic temperature, $\bar{T}$, using Eqns. 23, 24 and 25. Plot of the same silica concentration as a function of $\bar{T}$ (solid line). The slope of the curve now yields activation energies from 11 kcal/mol to 14 kcal/mol.

The earlier section discussed the simpler dependence of the rate on the amount of adsorbed hydrogen ions or hydroxyl ions on the mineral surface (e.g., using Eqn. 11). Some of the earlier work (KLINE and FOGLER, 1981a,b) already approached the catalysis by salts and pH, using adsorption isotherms. With the use of surface titration techniques as introduced to mineral dissolution rate studies by FURRER and STUMM (1986), the rates could be directly compared to the surface charge (and indirectly to the concentration of adsorbed ions). BLUM and LASAGA (1988) obtained a rather simple linear rate law for both olivine and albite when expressed in terms of the adsorbed hydrogen or hydroxyl ion concentration, i.e.,

$$\text{Rate} = k_{\text{other}} X_{\text{H+,ads}} \quad \text{(acid region)} \quad \text{and}$$

$$\text{Rate} = k_{\text{other}} X_{\text{OH-,ads}} \quad \text{(basic region)} \qquad (33)$$

where k_{other} represents all the other factors in Eqn. 11. Therefore, in their work, the exponent $n_{H+,ads}$ was 1. Kinetically, such a linear dependence can be explained by a reaction mechanism that consists of a sequence of slow hydrogen-ion-mediated hydrolysis steps (LASAGA, 1990). Interestingly enough, a recent study by BRADY and WALTHER (1992) finds the same dependence of the rate on $X^{1}_{\text{H+,ads}}$ for kaolinite and quartz.

Solution ionic strength has been shown to affect dissolution rates of quartz (KLINE and FOGLER, 1981a,b; DOVE and CRERAR, 1990; DOVE and ELSTON, 1992). Precipitation rates of quartz are also accelerated as ionic strength increases (HOSAKA and TAKI, 1981a,b; CORWIN and SWINNERTON 1951; LAUDISE, 1958). DOVE and CRERAR (1990) showed that the cation is important in controlling the reaction path of Si detachment and hence, the absolute dissolution rate.

Other solution components, such as Al, may also be an important catalyst or inhibitor to mineral reaction rates. For example, CHOU and WOLLAST (1985) suggested that the Al concentration was an important inhibitor, controlling the dissolution rate of albite in the dissolution plateau region. However, this conclusion must be modified because saturation state calculations were not made in their study.

The distinction between catalysis/inhibition and an effect due to $f(\Delta G_r)$ is a critical one to make, especially for species that directly affect ΔG_r. For example, although the solutions studied by CHOU and WOLLAST (1985) were not close to equilibrium, BURCH et al. (1993) showed that significant changes in albite dissolution rate occur out to undersaturations of −10 kcal/mol (using Eqn. 1 to define ΔG_r). Therefore, it is imperative to define by experimental work what is meant by far from equilibrium. This point raises an important consideration: to what extent is Al (or Si or Na) acting as a catalyst/inhibitor, and to what extent are the changes in Al

leading to changes in ΔG_r, which then is the primary cause to rate change via the $f(\Delta G_r)$ function.

A useful method to provide answers to this fundamental question is an isotach plot introduced into the mineral-solution kinetics literature by BURCH et al. (1993). Isotach plots are plots of constant growth rates contoured on an activity-activity diagram. NIELSEN and TOFT (1984) used isotach plots to show precipitation rate data for electrolyte salts. An important result of the form of Eqn. 8 is that if the rate law is only a function, $f(\Delta G_r)$, of the free energy of reaction, then the same growth (or dissolution) rate would be obtained under various solution compositions as long as the activity product remained the same. The shape of the isotachs can provide a first glimpse to the validity of the $f(\Delta G_r)$ function. If the rates are constant for constant ΔG_r, then the isotach plots should be straight lines with the slope determined by the stoichiometry of the mineral reaction. For example, in the case of fluorite growth, if the rate law (i.e., f) were such that

$$\text{Rate} = k_{\text{eff}}\Delta G^n, \tag{34}$$

where k_{eff} incorporates the other terms of Eqn. 8, then we have

$$\text{Rate} = k_{\text{eff}}\left[RT \ln\left(\frac{a_{\text{Ca}}a_{\text{F}}^2}{K_{\text{eq}}}\right)\right]^n. \tag{35}$$

Recall that in isotach plots the growth rate is fixed. Therefore, fixing the value of Rate in the last equation, the activity product can be solved for

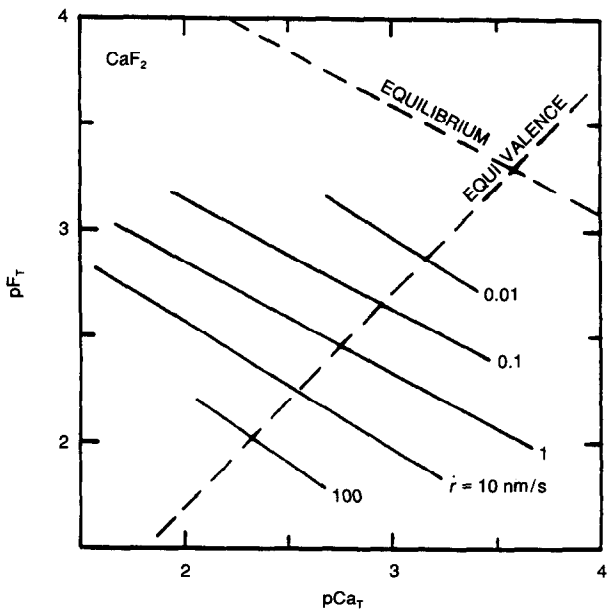

FIG. 13. Isotach plot of the dissolution rate of fluorite, CaF_2. Data and isotach from NIELSEN and TOFT (1984). The curves are contours of constant dissolution rate. $p\text{F} = -\log a_{\text{F}^-}$ and $p\text{Ca} = -\log a_{\text{Ca}^{2+}}$. Equilibrium line represents the zero reaction rate and has a slope of $-\frac{1}{2}$ based on the stoichiometry of the fluorite dissolution (Eqn. 29 with $C = K_{eq}$).

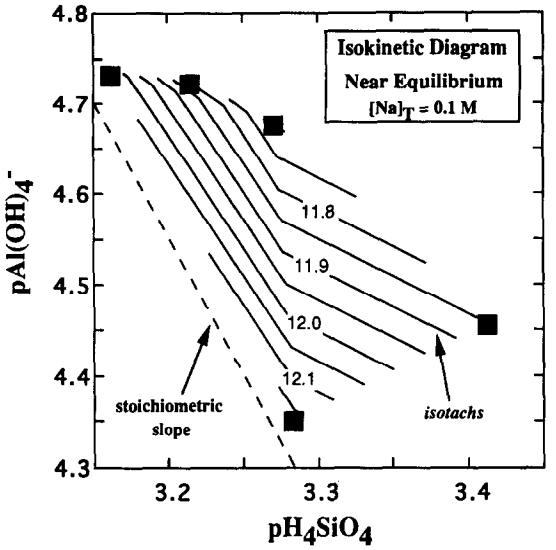

FIG. 14. Isotach plot of the dissolution rate data of albite at 80°C and pH 8.8 from BURCH et al. (1993). Isotachs approach the solubility slope for albite (——), suggesting a true rate dependence on ΔG_r. $p(\ ) = -\log$ activity of $(\ )$.

$$a_{\text{Ca}}a_{\text{F}}^2 = K_{\text{eq}} \exp\left(\frac{(\text{Rate}/k_{\text{eff}})^{1/n}}{RT}\right) = C \quad \text{constant.} \tag{36}$$

Taking logarithms of both sides,

$$\ln a_{\text{F}} = \tfrac{1}{2} \ln C - \tfrac{1}{2} \ln a_{\text{Ca}}. \tag{37}$$

As a result an isotach plot for fluorite which has pF vs. pCa as axes ($\text{pF} = -\log(a_F)$ and $p\text{Ca} = -\log(a_{Ca})$) should lead to straight lines of constant slope $= -\frac{1}{2}$ (regardless of the value of n). Such an isotach plot is shown in Fig. 13. Note the dashed line (of slope $-\frac{1}{2}$) denoting the equilibrium conditions for fluorite. Indeed, the isotach curves are very close to straight lines, with slope $-\frac{1}{2}$. In this case, the isotach plots support the idea that one needs only the function f to describe the variation of the rate law with solution composition.

Figure 14 (from BURCH et al., 1993) gives some preliminary isotach plots for the albite dissolution rate. In this case, the activity of Na in solution was maintained constant, while the activity of both Si and Al was varied in a series of experiments. Therefore, the isotach plots use pAl and pSi as the axes. Note that the isotachs are indeed fairly close to the line predicted by stoichiometry (3:1 Si:Al), just as in the case of CaF_2 discussed above. Close adherence to the line suggests $f(\Delta G)$ is controlling the rate. For example, if Al was the dominant inhibitor, then the isotachs should be horizontal lines that depend mostly on the Al content of the solutions. Use of isotach plots should be important in future water-rock kinetic work to unravel the ΔG_r effect from possible catalytic or inhibitory effects of different solution species. These isotach plots, then, are essential to the extraction of the general rate laws needed in weathering studies such as Eqn. 8 or 11.

Global Cycles and Weathering

The rate laws for water-rock interactions are central to the quantification of global geochemical cycles. In particular, the

geological control of CO_2 in the atmosphere depends on the rate of weathering of silicates in the surface of the Earth (BERNER et al., 1983; LASAGA et al., 1985). As noted in the earlier work, it is not the total weathering that affects CO_2, but the weathering of silicates in particular. Thus, the weathering of carbonates will use up CO_2 but give it back again upon precipitation of calcite in the oceans. However, the weathering of silicates not only uses up CO_2, but the CO_2 is not fully recovered when carbonates are also precipitated in the oceans. For example, in the weathering of feldspar to kaolinite,

$$CaAl_2Si_2O_8 + 2CO_2 + 3H_2O \Rightarrow$$
$$Ca^{2+} + Al_2Si_2O_5(OH)_4 + 2HCO_3^-; \quad (38)$$

the subsequent precipitation of calcium carbonate in the oceans:

$$Ca^{2+} + 2HCO_3^- \Rightarrow CaCO_3 + H_2O + CO_2, \quad (39)$$

leads to a net loss of one mole of CO_2 per mole of feldspar dissolved. Similarly, the overall reaction for the weathering of a pyroxene to make carbonate is given by

$$CaSiO_3 + CO_2 + 2H_2O \Rightarrow CaCO_3 + H_4SiO_4. \quad (40)$$

Therefore, understanding of the controls on the global weathering rate of silicates is essential to a quantification of the global geochemical cycle of C, as well as its effect on paleoclimate. As discussed in the earlier part of this paper, there has been much progress in our understanding of water-rock kinetics. These results should be introduced in the treatment of global cycles.

An example of the role of weathering in the global models is shown by the BLAG treatment. In this treatment, the negative feedback on the CO_2 content of the atmosphere was provided by the effect of CO_2 on temperature. Increases in CO_2 led to increases in temperature. Increases in temperature, in turn, led to an increase in the silicate weathering rate and in the hydrologic cycle (i.e., in runoff from continents). The increase in weathering rate due to temperature was obtained from field data, and the runoff was obtained from various GCM (global climate model) calculations (e.g., for GCM references see PITCHER et al., 1983; RAMANATHAN et al. 1983; WILLIAMSON et al., 1987). The result was the feedback function $f_B(CO_2)$. $f_B(CO_2)$ is defined to be 1 for the atmospheric CO_2 content of today and increases as the CO_2 content increases above the value of today (see later). In addition, the changes in land area were taken to lead to concomitant changes in the weathering rate, i.e., the rate varied as the ratio, f_A, of land area in the past to the current value,

$$f_A \equiv \frac{\text{Area}(t)}{\text{Area(today)}}. \quad (41)$$

Therefore, the total uptake of CO_2 by silicate weathering varied as $f_A(t) f_B(CO_2)$. This sink rate was balanced, at steady-state, by the source term, which was dominated by the rate of tectonic magmatism and metamorphism, f_{SR};

$$f_{SR} \equiv \frac{\text{Total Spreading Rate}(t)}{\text{Total Spreading Rate(today)}}. \quad (42)$$

Altogether, then, the steady-state balance of CO_2 in the atmosphere leads to the simple equation

$$f_A f_B(CO_2) = f_{SR}. \quad (43)$$

As pointed out by other workers (KASTING, 1984; BRADY, 1991), this simple equation can be solved for CO_2 through time (and hence an indication of paleoclimate). While later BLAG models (LASAGA et al., 1985) cannot be adequately treated by Eqn. 43 (e.g., it would force ignoring organic C), Eqn. 43 does serve the purpose of emphasizing the key role of weathering. For example, some workers have argued that changing the land area in nonmountainous regions does not lead to a significant change in the weathering rate, because the lowlands contain only leached minerals such as kaolinite (i.e., $f_A = 1$). Others have argued that the role of temperature in f_B is minor, and that the rate of uplift of mountains such as the Himalayas are the most important parameters in the weathering equation. We would like to address some of these issues here.

Many estimates of the global chemical denudation rate have been given in recent years (STALLARD, 1988; HOLLAND, 1978; MEYBECK, 1988). It is generally agreed that physical weathering is about six times larger than chemical weathering. Chemical weathering, however, is the important parameter in the chemical fluxes of CO_2 within global cycles. The chemical denudation rate is given as 0.014 mm/y by MEYBECK (1988); STALLARD (1988) gives a range of 0.005 to 0.03 mm/y for the continental shields and sediments; HOLLAND (1978) puts the global estimate as 0.008 mm/y.

An interesting gedanken calculation of a chemical denudation rate would be based on a solid feldspar continent. The recent dissolution rate of feldspar far from equilibrium, k_+, is around 1×10^{-16} mol/cm^2/s at 25°C and near neutral pH (CHOU and WOLLAST, 1984; BLUM and LASAGA, 1988). Therefore, the retreat of the surface due to dissolution would simply be given by

$$\text{Denudation Rate} = k_+ \bar{V}, \quad (44)$$

where $\bar{V}$ is the molar volume of feldspars (100 cm^3/mol). In this case, the denudation rate is calculated to be 3×10^{-6} mm/y. Clearly, such a rate is far too low.

A much better model (Fig. 15) would include the depth of the regolith or weathering zone. If the mean size of weath-

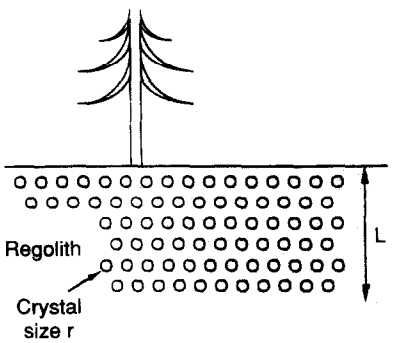

FIG. 15. Simple model for global chemical weathering. The mean regolith depth is labeled, L. The reactive minerals are taken as having a homogeneous crystal size, r.

erable silicates (e.g., the feldspars) is r and the percent modal abundance is x%, then the area of mineral is given by (LASAGA, 1984):

$$A = \frac{3x}{100r} \text{ cm}^2/\text{cm}^3 \text{ rock.} \quad (45)$$

If the global depth of the regolith is given by L and the surface area undergoing weathering is A_s, then the total volume exposed to chemical weathering is $A_s L$ and the net volume loss due to weathering is

$$\frac{dV}{dt} = A_s \frac{dL}{dt} = k_+ A L A_s \bar{V} \quad (46)$$

or

$$\frac{dL}{dt} = \frac{k_+ 3xL\bar{V}}{100r}. \quad (47)$$

Using the values $k_+ = 1 \times 10^{-16}$ mol/cm^2/s, $r = 0.1$ cm, $x = 20$%, and $L = 5$ m, leads to

$$\frac{dL}{dt} = 0.009 \text{ mm/y}, \quad (48)$$

which agrees with estimates of global chemical weathering rates by others discussed above (STALLARD, 1988; HOLLAND, 1978; MEYBECK, 1988). We do not expect the value of L to be more than an order of magnitude bigger (50 m) or more than an order of magnitude smaller (0.5 m). The calculation shows that the experimental rate data, such as discussed in this paper, is consistent with the geochemical field observations.

BERNER et al. (1983) obtain a global use of CO_2 by Ca-Mg silicate chemical weathering of 5.7×10^{12} mol CO_2/y (similar values have been used by BERNER, 1990, 1991). One can compute the area needed to produce this uptake of CO_2, using the rate of dissolution of wollastonite at 25°C and pH = 5 (RIMSTIDT and DOVE, 1986), i.e., 6×10^{-13} mol/cm^2/s (the anorthite rate is also similar—see Table 1). The net rate of CO_2 uptake is based on a reaction such as in Eqn. 40. Therefore, to dissolve 5.7×10^{12} mol of $CaSiO_3$ in a year (i.e., 1.8×10^5 mol/s) requires a wollastonite area of 3×10^{17} cm^2. A rock containing 20% $CaSiO_3$, with a mean size of 1 mm yields a surface area of 6 cm^2/cm^3 rock (Eqn. 48). Therefore, one would need 5×10^{16} cm^3 of reactive rock. The total land area of continents (with external drainage) is 1×10^{18} cm^2 (HOLLAND, 1978). Twenty-five percent of the land area is underlain by igneous and metamorphic rocks (HOLLAND, 1978). Even if only 10% of this last area (i.e., 2.5% of the total area) contained mafic or high grade metamorphic rocks, then the land area available would be 2.5×10^{16} cm^2. To produce the necessary reactive rock volume, only a depth of 2 cm would be required. Of course, for different temperatures the depth would vary. Using an activation energy of 19 kcal/mol (RIMSTIDT and DOVE, 1986), the depth would increase to 11 cm at a temperature of 10°C. Clearly, the laboratory rates can accomodate the types of weathering rates required in the global change models. In fact, the kinetic data can provide further checks on the type of assumptions being made in global models, as will be discussed in the next section.

Another calculation relevant to the rate of generation of lateritic soils involves the movement of a granitic (feldspar) interface under the action of flow of water. Using a flow rate of 1–100 m/y, dispersion/diffusion coefficient of 10^{-4} cm^2/s, and the dissolution rate for feldspar, the result of a one-dimensional coupled fluid flow and chemical reaction calculation is given in Fig. 16 (the next section discusses these calculations further). The plot is showing the relative concentration of silica (as C_{Si}/C_{ey}). The first curve in Fig. 16a shows the initial steady-state solution profile, reaching equilibrium with the feldspar in about 20 m. As the dissolution of the feldspar in the top region proceeds, the interface between fresh feldspar and weathering zone retreats. The second curve in Fig. 16 shows the movement. Note that the interface (saprolite-granite) has moved about 20 m in 2 million y or 10 mm/1000 y. It is interesting to compare this number with the rate of saprolite formation from a granite observed in nature and given by TARDY (1969) as 34 mm/1000 y or the rate of VELBEL (1985) for saprolite formation of 37 mm/1000 y (see also discussion in NAHON, 1991). For flow rates of 10 and 1 m/y, the advance (Fig. 16b,c) is 2 m and 0.4 m in 2 million y.

Water-Rock Kinetics, and Concentration vs. Runoff in Rivers

Ultimately, the chemical fluxes obtained from the dissolved load of all the rivers of the world give the best estimate of the chemical denudation processes. The problem with quantifying the river data, however, is that no small set of rivers dominate the numbers in the global calculation.

The data for the various elements show different patterns in the plots of concentration vs. runoff (HOLLAND, 1978). Some elements such as chloride exhibit a simple inverse proportionality to runoff. The dissolved species of more interest to the global silicate weathering such as bicarbonate or silica, however, exhibit a more complex pattern. Figure 17 (from BLUTH and KUMP, 1994) illustrates a typical plot for silica. (BLUTH and KUMP, 1994, (this issue) for an extensive discussion of the recent data). This plot of silica in rivers vs. runoff is very important in the global change models because it enters into many of the assumptions about weathering feedbacks (BERNER et al., 1983; BERNER, 1990, 1991). An inverse proportionality to runoff can be understood by a simple model which relates the runoff to the flow rate of solutions through the regolith. If the conditions are such that the dissolution of silicates (or other solids) lie in the dissolution plateau region, then the rate of change of the concentration is given by

$$\frac{dc}{dt} = \frac{A}{V} k_+, \quad (49)$$

where A/V is the kinetic water-rock ratio. The concentrations of elements that are measured in rivers and streams are the result of the integrated hydrologic paths of different packets of solution through the regolith. The mean distance travelled by a solution through the regolith, X_{reg}, becomes an important parameter, related to the mean regolith depth, L. The other parameter is the mean flow rate, v, of the solution through the regolith. This flow rate should correlate strongly with the

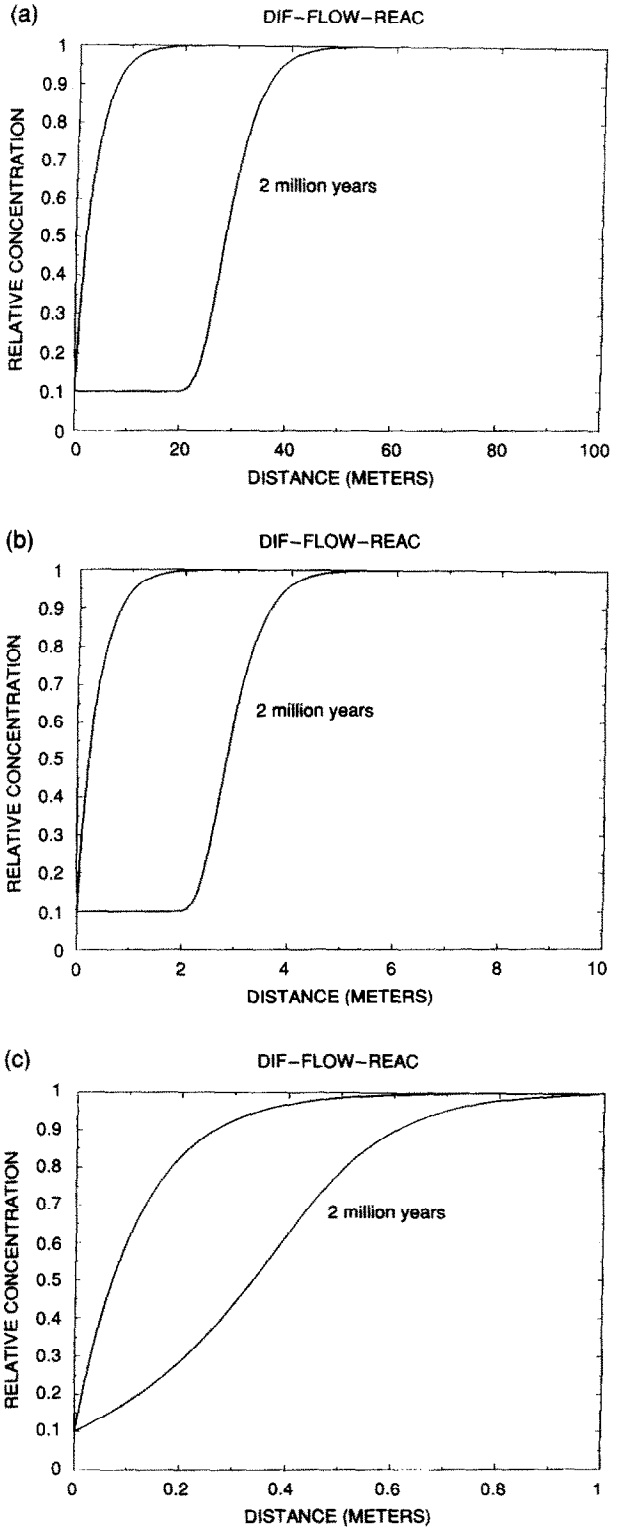

FIG. 16. Chemical evolution of a reactive feldspar (granite) system. The calculation assumes a simple linear rate law (e.g., as in the mass transfer section) with rate constant obtained from recent rate data. The surface area of the reacting mineral is evaluated from the abundance and is updated as mineral dissolves. Calculation assumes porosity of 0.001, dispersion coefficient of 10^{-4} cm^2/s, and an initial feldspar radius of 1 mm and 4.8×10^7 grains feldspar/m^3 rock. The one-dimensional fluid flow-reaction equations were solved numerically. In each case, the first curve is the initial steady-state (achieved in a few years) concentration profile of $c_{Si}/c_{Si,eq}$ in the water-saturated rock. The second curve shows the new steady state 2 million years later (as the original feldspar minerals have been dissolved away from the rock). The movement of the reaction front corresponds to the movement of a saprolitic boundary. (a) $v = 100$ m/y (b) $v = 10$ m/y (c) $v = 1$ m/y.

runoff. In the simple case mentioned above, the dissolution rate is constant, and thus in the time needed to reach the streams or rivers, X_{reg}/v, the concentration that results is given by

$$c = \frac{A}{V} k_+ \frac{X_{reg}}{v}. \quad (50)$$

Obviously, this simple hydrologic model would predict a 1:1 inverse relation between concentration and runoff (by analogy to v). Such a relation was observed for some dissolved elements by HOLLAND (1978).

The new kinetic data discussed in this paper, however, suggests that for most silicates the strong nonlinearity of the $f(\Delta G_r)$ function would lead to a departure from the dissolution plateau at significant undersaturations. Once the dissolution rate depends on the solution composition, the relation between concentration and runoff changes dramatically and approaches a line with near zero slope in the limit that equilibrium is approached.

We can use the measured decrease in albite dissolution rate with approach to equilibrium (Burch et al., 1993) to understand the global plots of Si vs. runoff (BLUTH and KUMP, 1994; HOLLAND, 1978). Calculations were carried out, keeping track of solution composition and including the kinetics of precipitation and dissolution for the proto-granite system, i.e., feldspar, gibbsite, mica, and kaolinite. The full rate laws (e.g., Eqn. 6) were used for all minerals in the calculation. The resulting concentration of silica at different values of X_{reg}, and for different initial pH are shown as a function of runoff (flow rate) in Figs. 18 and 19. It is interesting to note the strong similarity to the classic HOLLAND (1978) plots of silica vs. runoff. These results indicate that chemical kinetics can account for the field observations of natural streams and rivers.

The results of Figs. 18 and 19 all stem from the very important decrease in the rate as ΔG_{crit} is reached. Without knowledge of the $f(\Delta G_r)$, the rates would have been assumed to be much less dependent on the solution composition (for example, the pH effect on rates is minimal in the 5–7 pH range of many of these reactions in nature) and the predicted concentration vs. runoff curve would have to be very close to an inverse proportionality. The value of ΔG_{crit} provides a new guideline for the end of the dissolution plateau and thus for the bending of the concentration vs. runoff data away from the 1:1 inverse proportionality. Note that, in the event that nature would have been governed by the inverse law, there would have been no dependence of the silicate weathering rate on runoff, i.e., the BLAG feedback on the hydrologic cycle would not have been there. As runoff increases, the concentration of silica, in this model, decreases and hence the total global flux of silica (i.e., runoff × conc.) would remain the same.

Comparison of Figs. 17 and 19 reveal that the kinetic rate laws can simulate the type of variation observed in natural streams. However, it is clear that, again, realistic models need

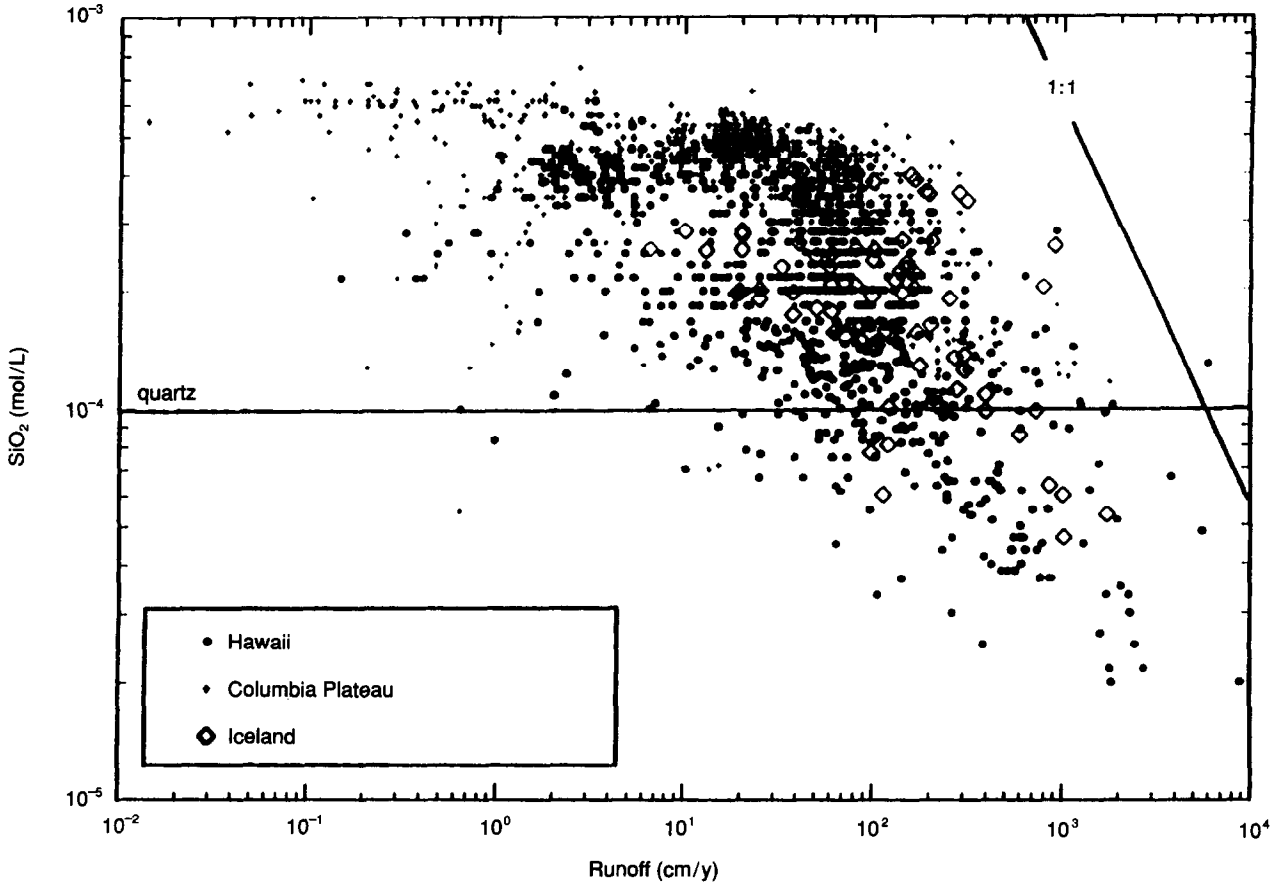

FIG. 17. Concentration of silica vs. runoff for rivers draining basaltic terrains in Hawaii, the Columbia Plateau and Iceland. Plot from BLUTH and KUMP (1994). Quartz line is the equilibrium line at 25°C.

to incorporate more sophisticated treatments of variations in fluid flow velocities within natural settings, as well as variations in rock types and temperature fields (STEEFEL and LASAGA, 1992, 1994). The main point of the comparison is to emphasize the possible role of inorganic mineral kinetics in controlling the silica content and to underscore the need to quantitatively explore the linkage between the mineral surface rate laws discussed in the earlier part of this paper and the geochemical field observations.

There are two other features relating chemical kinetics of weathering and global cycles. First, some workers (RAYMO and RUDDIMAN, 1992) have invoked the rise of mountains as leading to an increase in weathering rate. The idea is not to violate the Arrhenius law (which would be physically chemically quite incorrect) but to invoke the crushing of fresh material (increase in surface area) and the exposure of fresh material due to tectonic processes to increased orographic rainfall on the windward side of mountains as leading not only to physical erosion but to increased chemical weathering. In particular, the rise of the Himalayas has been linked to an increase in chemical weathering of silicates during the past 30–40 million years.

The quantification of these claims needs quite a bit more work. First, it is clear that—all other things being equal—an increase in the surface area of a mineral will lead to an increase in the total dissolution rate of the mineral (although not to an increase in the rate of dissappearance of the mineral grain; see LASAGA, 1984). In addition, increased rainfall may lead to increased total chemical weathering flux (see earlier section). However, many chemical and physical factors are coupled in the weathering system of an active mountainous region such as the Himalayas. In fact, many workers (HOLLAND, 1978; BERNER and BERNER, 1987) have noted that there is no correlation between chemical denudation rate and relief, such as is clearly evident between physical erosion and relief. This lack of a relation is not only true for total chemical erosion, but also for silicate chemical erosion. The best indicator for silicate weathering is not HCO_3^-, but dissolved H_4SiO_4 in the streams. Figure 20a shows the clear relation between sediment yield and mean continental elevation (such as shown by HOLLAND, 1978). Figure 20b and c give the mean silica concentration and the total silica discharge from continents as a function of mean continental elevation. Excluding evaporites and carbonates by use of the dissolved silica content, Fig. 20 illustrates this lack of correlation. Note that the data on Asia of MEYBECK (1979) exclude the large flows occurring in the New Zealand, Japanese, and Indonesian rivers. In a global sense, the influence of even the rivers draining the Himalayas is diluted by the large amount of drainage from many rivers. As HOLLAND (1978) and others have pointed out, the cumulative discharge from the top twenty rivers is only 31% of the total discharge from all the

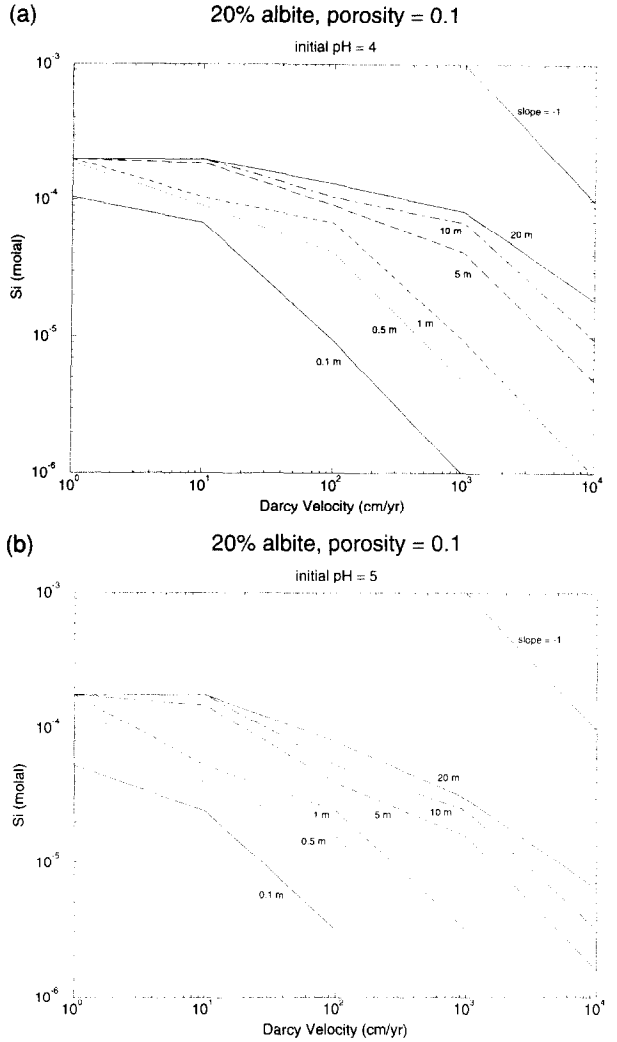

FIG. 18. Plot of calculated silica concentrations in solutions travelling with different velocities (runoff) through different net distances in the regolith. Calculations use the full dissolution/precipitation rate laws obtained for feldspar, gibbsite, kaolinite, and mica. (a) Calculations use initial pH = 4. (b) Calculations use initial pH = 5.

measured rivers of the world. The net dissolved silica output from the Yangtze, Ganges, Brahmaputra, and Mekong rivers is only 6% of the total dissolved silica output.

To make sense of the lack of correlation of the chemical weathering data and the source of fresh rock coming from the rise of the Himalayas, one must link the weathering rate (e.g., Table 1) to the physical transport rate. An interesting calculation can be made taking the total sediment yield (HOLLAND, 1978):

$$\text{Sediment Yield} = F_s = 2 \times 10^{16}\ \text{g/y}. \qquad (51)$$

As Fig. 21 illustrates, the continents may be modeled as a weatherable regolith of depth, L. In this case, a residence time for the physically transported material (i.e., a regolith residence time) can be calculated as

$$\tau_{\text{physical weathering}} = \frac{A_{\text{cont}}\rho L(1-\phi)}{F_s}, \qquad (52)$$

where A_{cont} is the continental area with external drainage (about two-thirds of total land area), ϕ is the average porosity, and ρ is the sediment density (g/cm^3). This leads to the value

$$\tau_{\text{physical weathering}} = \frac{1 \times 10^8\ \text{cm}^2\ 2.7\ 1000\ \text{cm}\ 0.8}{2 \times 10^{16}\ \text{g/y}}$$

$$= 108{,}000\ \text{years}. \qquad (53)$$

This number would include the transport of material in large drainage areas such as the Amazon basin or the Mississippi drainage basin. Most workers believe that the transport of material from the Himalayas to the Bengal fan is relatively fast. If the time involved drops to tens of thousands of years, the time would be short for significant chemical weathering of many silicates including pyroxenes, biotites, and feldspars (e.g., see Table 1). The earlier data (e.g., Table 1 and LASAGA, 1984) are based on dissolution into a highly dilute solution. Our recent data (cited earlier) indicate that the rates will

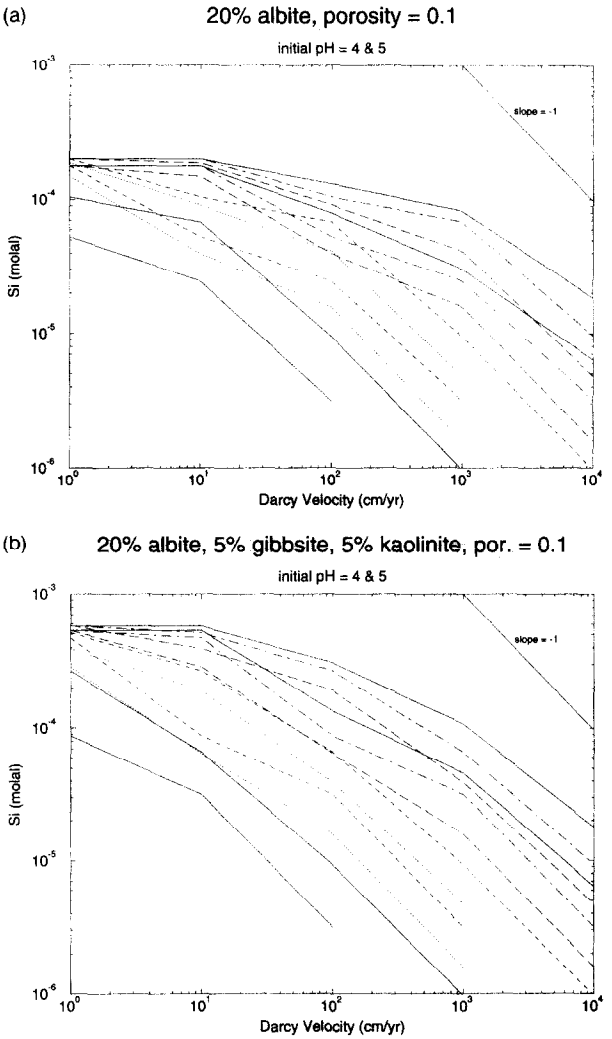

FIG. 19. (a) Combination of plots in Fig. 18. The resulting silica concentration vs. Darcy velocity (runoff) plot should be compared with that in Fig. 17. Note the approach to $1/v$ behavior at high velocities (high runoff) in a manner similar to the field observations. (b) Same as (a), but with rock initially containing 20% albite, 5% gibbsite, and 5% kaolinite.

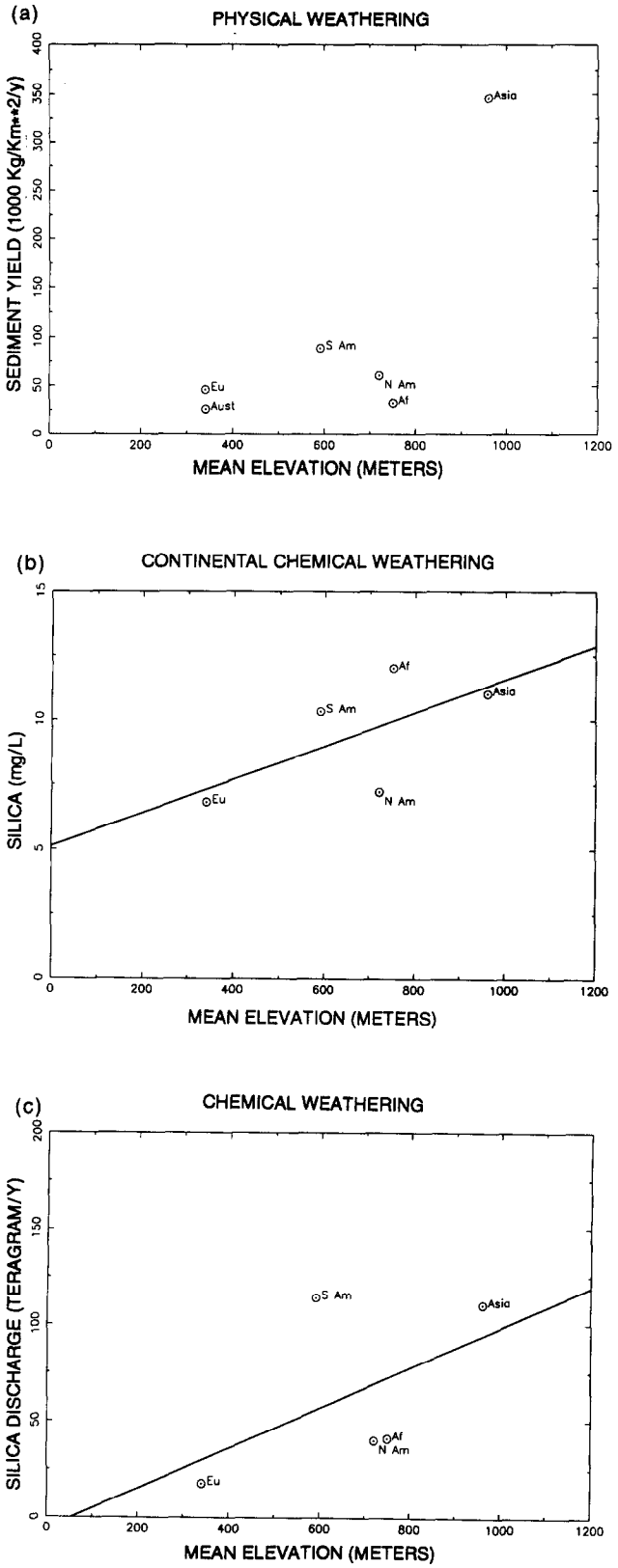

FIG. 20. (a) Plot of total sediment yield for each continent as a function of the mean continent elevation. (b) Plot of average dissolved silica concentration versus mean elevation for the different continents. (c) Plot of total silica discharge into the oceans for the different continents as a function of mean continent elevation. (data from MEYBECK, 1979; BERNER and BERNER, 1987).

drop by an order of magnitude or more, if significant interaction with solutions takes place. If the mineral grains were crushed to a very fine grain size (e.g., 10 μ), then the time to dissolve could be shortened to values shorter than the $\tau_{physical}$ values above. However, high reliefs usually lead to the transport of more coarser-grained material towards the base level (e.g., estuaries, continental shelfs, etc.) of the streams.

Another important consideration is the land area term, f_A, used in the BLAG and similar formulations. The work done on the Amazon (STALLARD and EDMOND, 1983; STALLARD, 1988) has emphasized that most of the solutes in the Amazon come from the Andes, and little comes from the low-lands of the Amazon basin. Extrapolating to all the continents, the idea is that fluctuations in sea level, leading to changes in land area, will only affect areas that are so thoroughly leached in cations that the uptake of CO_2 will not be affected. For example, the conversion of kaolinite to gibbsite does not require CO_2:

$$Al_2Si_2O_5(OH)_4 + 5H_2O \rightarrow 2Al(OH)_3 + 2H_4SiO_4. \quad (54)$$

There are a couple of problems with this scenario. First, there are portions of the shelf and lowlands that are not either carbonates or bauxite deposits. Second, changes in sea level will lead to a change in the groundwater hydrologic system. Even in systems which have leached zones, the deeper portions contain clays such as smectites that do have cations and will use up CO_2. A change in the hydrologic system can lead to the dissolution of these smectites or even saprolites.

Therefore, the actual feedback mechanism is probably somewhere in between the BLAG f_A term and assuming no effect (which is almost surely also wrong). To show the effects of changing the f_A on the BLAG type calculations, the land area variation (based on BARRON et al., 1980; RONOV, 1976) and the f_{SR} term derived from the Vail sea level curve (GAFFIN, 1987) are used in evaluating the variation of CO_2 through time (See Fig. 22a,b).

The CO_2 levels were obtained from solving the very simplified BLAG formulation discussed earlier,

$$f_B(CO_2) = \frac{f_{SR}(t)}{f_A(t)}. \quad (55)$$

The very important function $f_B(CO_2)$ still is not precisely known, although the kind of water-rock kinetic data discussed in this paper should contribute in a major way to constraining the function. Based on the earlier discussion on activation energies, the original BLAG function is still being used, except as modified by a Michaelis Menten term:

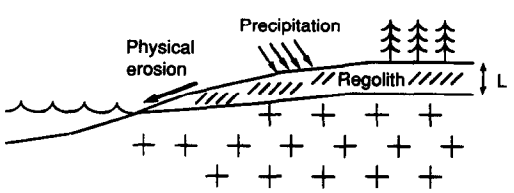

FIG. 21. Simple model to calculate the mean residence time of regolith minerals in continents. L is the global mean regolith depth. The residence time depends on the net transport of primary minerals and weathered products principally by physical erosion to the continental shelves.

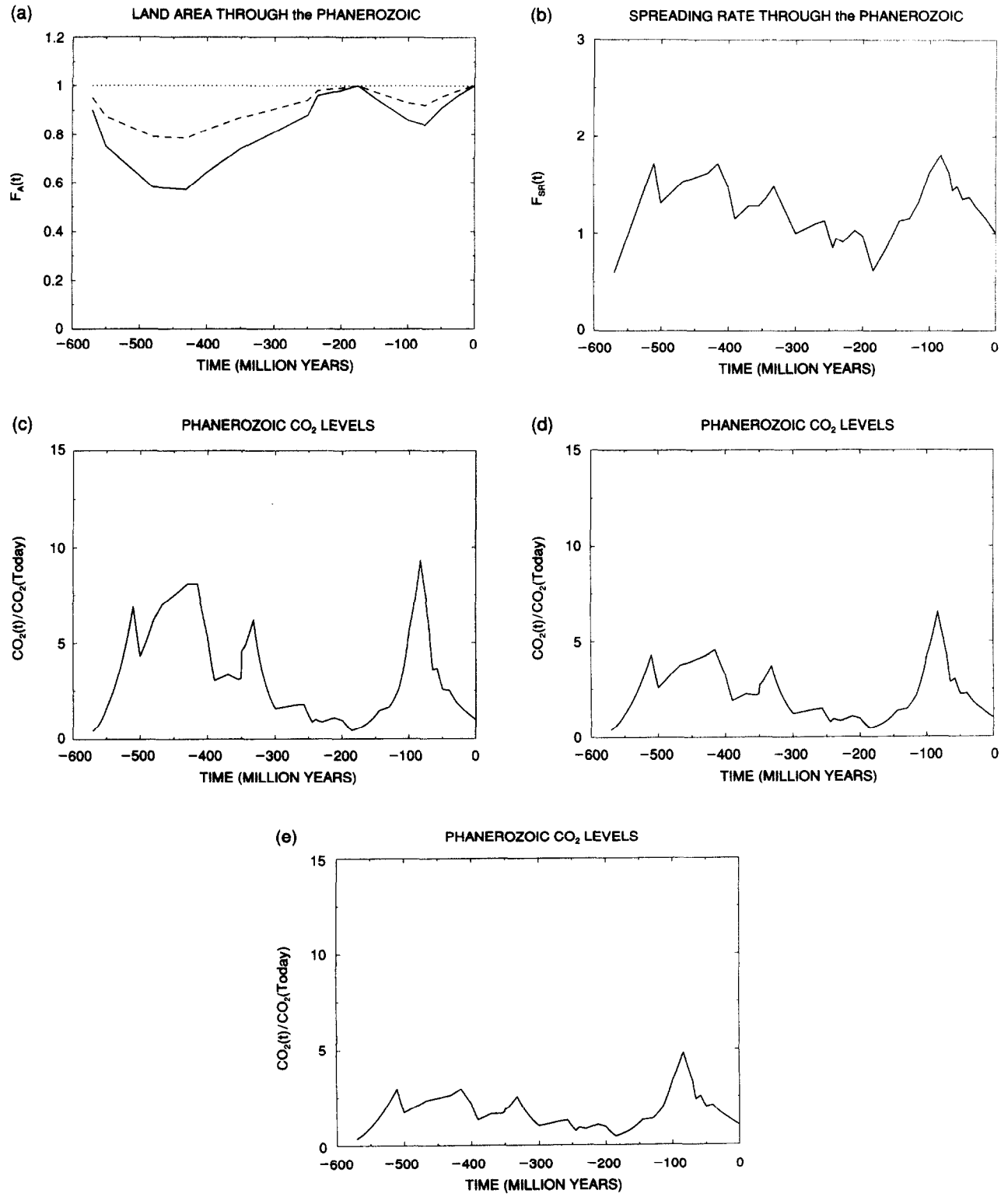

FIG. 22. Calculation of BLAG-type temperature curve for the Phanerozoic. CO_2 is calculated from solving Eqn. 31, once f_A and f_{SR} are known at any one time. The f_B (CO_2) function used is modified from that of BERNER et al. (1983). (a) Different values of the f_A curve as a function of time: (——) f_A = Land Area(t)/Land Area (today); (------) f_A = 1 + ½ (Area(t)/Area (today) − 1); (· · · ·) f_A = 1. (Data from RONOV (1976) and BARRON et al. (1980)). (b) Variation of $f_{SR}(t)$ used in the calculation (derived from the Vail sea level curve (GAFFIN, 1987). (c) Case which assumes that f_A = Land Area(t)/Land Area (today) (i.e., the BLAG case). (d) Case which assumes that f_A = 1 + ½ (Land Area(t)/Land Area (today) − 1). (e) Case which assumes f_A = 1.

$$f_B(CO_2) = [1.0 + 0.251 \ln X + 0.0154(\ln X)^2]\left[\frac{1.5X}{0.5 + X}\right]^{0.75}, \quad (56)$$

where

$$X \equiv \frac{CO_2(t)}{CO_2(\text{today})}. \quad (57)$$

The first term in Eqn. 56 is the BLAG feedback function (BERNER et al., 1983). BRADY (1991) corrected this feedback to a higher activation energy of 15 kcal/mol, based on the extraction of 9 kcal/mol for the activation energy of the river data. However, the earlier section discussed the compatibility of such an activation energy with the higher activation energies obtained by the water-rock kinetic data. The second term in Eqn. 56 represents a Michaelis Menten correction (see VOLK, 1987; BERNER, 1991). We have modified the term used in BERNER (1991) to make the overall dependence be linear with CO_2, as the CO_2 values become very small (hence the 0.75 exponent).

Obviously a variety of f_B functions can be used in these type of models. Nonetheless, the main point that we want to make here is the importance of the land area term, f_A. Therefore, in calculating the CO_2 levels, three different f_A curves were used as shown in Fig. 22a:

$$f_A = 1, \quad (58)$$

$$f_A = \frac{\text{Area}(t)}{\text{Area}(\text{today})}, \quad (59)$$

$$f_A = 1 + \frac{1}{2}\left(\frac{\text{Area}(t)}{\text{Area}(\text{today})} - 1\right). \quad (60)$$

The results are shown in Fig. 22c–e. The overall variation in CO_2 throughout the Phanerozoic is similar to that from other calculations (LASAGA, et al., 1985; BERNER, 1990, 1991), with important increases in the Cretaceous and the Cambro-Ordovician and cooling (low CO_2) during the Permo-Carboniferous period. These variations are in broad accord with the climatic record and have been calculated by others as well (BERNER et al., 1983; LASAGA et al., 1985; BERNER, 1990, 1991). However, note the important effect of the land area term in modulating the absolute magnitude of the fluctuation in CO_2, especially in the Paleozoic. Future work needs to go back to paleogeographic maps and, based on the distribution of rock types as a function of elevation, quantify the proper land area factor to use in global cycles models. The story on the role of f_A is not over yet.

CONCLUSIONS

The treatment of water-rock kinetics requires that full rate laws be obtained for each of the reacting minerals. Kinetic effects can be expected to change drastically the usual interpretation of activity-activity diagrams. Furthermore, any quantitative treatments of coupled reaction and fluid flow in diagenesis, weathering, or hydrothermal systems must be based on full rate laws. Such rate laws necessitate that the effects of temperature, pH, and solution composition be integrated with the effects of changing the saturation state to achieve a complete picture. The emerging results from recent experiments suggest that the variation of the rate with saturation state is much more complex than anticipated. The presence of a surface transition in the mechanism of dissolution leads to highly nonlinear variations of the rate with ΔG_r. Such surface effects have been tentatively identified as stemming from the energetic role of dislocation defects on the surface of the minerals.

A new full rate law was proposed that explicitly incorporates the effect of ΔG_r, as well as that of temperature and adsorption of H^+, OH^-, and other ions. The pH effect on activation energies should be approached from such a full rate law. The apparent activation energies from mineral dissolution seem to follow a compensation law. The universal temperature is such that most mineral rates would become more similar as the temperature increases. The comparison of activation energies in field observations requires that a recalculation be made of the kinetic average temperature, as opposed to the average temperature. Such corrections, usually ignored in the past, can increase the activation energies by several kcal/mol.

The experimental data can account quite well for many of the observations in global chemical weathering. Not only can the experimental data predict the correct stability ordering of the minerals, but also quantitatively account for the magnitude of the terms. In addition, the new experimental data can explain the variation of silica in rivers worldwide as a function of runoff, without the need of recourse to an equilibrium model. The relationship between continental elevation and chemical weathering is shown to be much less cogent than that between elevation and physical weathering. The residence times for transport of debris from high altitudes may be fast, compared to the time required for chemical reaction (e.g., Table 1). Finally, the new understanding of the kinetics of water-rock interactions can help to formulate better the geochemical cycles models for CO_2, including the function, $f_B(CO_2)$, used in BLAG, as well as the role of land area in the overall chemical weathering rate.

Acknowledgments—The authors would like to gratefully acknowledge financial support through the Branch of Energy Science of the Department of Energy (grant DE-FG02-90-ER14153). In addition, the authors would like to acknowledge funding from the American Chemical Society (PRF 22364-AC2) and the National Science Foundation (NSF EAR 9017976). The authors would also like to gratefully acknowledge thorough reviews by Bill Murphy, Susan Brantley, Tom Wolery, and anonymous reviewer.

Editorial handling: H. Ohmoto

REFERENCES

AAGAARD P. and H. C. HELGESON (1982) Thermodynamic and kinetic constraints on reaction rates among minerals and aqueous solutions. I. Theoretical Considerations. *Amer. J. Sci.* **282**, 237–285.

AMRHEIN C. and SUAREZ D. L. (1988) The use of a surface complexation model to describe the kinetics of ligand-promoted dissolution of anorthite. *Geochim. Cosmochim. Acta* **52**, 2785–2793.

BALES R. C. and MORGAN J. J. (1985) Dissolution kinetics of chrysotile at pH 7 to 10. *Geochim. Cosmochim. Acta* **49**, 2281–2288.

BARRON E. J., SLOAN J. L., and HARRISON C. G. A. (1980) Potential significance of land-sea distribution and surface albedo variations

as a climatic forcing factor: 180 my to the present. *Paleogeogr. Paleoclimatol. Paleo.* **30,** 17–40.

BERNER E. K. and BERNER R. A. (1987) *The Global Water Cycle: Geochemistry and Environment.* Prentice Hall.

BERNER R. A. (1990) Atmospheric carbon dioxide levels over Phanerozoic time. *Science* **249,** 1382–1386.

BERNER R. A. (1991) A model for atmospheric CO_2 over Phanerozoic time. *Amer. J. Sci.* **291,** 339–376.

BERNER R. A. and MORSE J. W. (1974) Dissolution kinetics of calcium carbonate in sea water; IV, Theory of calcite dissolution. *Amer. J. Sci.* **274,** 103–134.

BERNER R. A., LASAGA A. C., and GARRELS R. M. (1983) The carbonate-silicate geochemical cycle and its effect on atmospheric carbon dioxide over the past 100 Million Years. *Amer. J. Sci.* **283,** 641–683.

BLOOM P. R. and ERICH M. S. (1987) Effect of solution composition on the rate and mechanisms of gibbsite dissolution in acid solutions. *Soil Sci.* **51,** 1131–1136.

BLUM A. E. and LASAGA A. C. (1987) Monte Carlo simulations of surface reaction rate laws. In *Aquatic Surface Chemistry: Chemical Processes at the Particle-Water Interface* (ed. W. STUMM), pp. 255–292. Wiley.

BLUM A. E. and LASAGA A. C. (1988) Role of surface speciation in the low-temperature dissolution of minerals. *Nature* **331,** 431–433.

BLUM A. E. and LASAGA A. C. (1991) The role of surface speciation in the dissolution of albite. *Geochim. Cosmochim. Acta* **55,** 2193–2201.

BLUM A. E., YUND R. A., and LASAGA A. C. (1990) The effect of dislocation density on the dissolution rate of quartz. *Geochim. Cosmochim. Acta* **54,** 283–297.

BLUTH G. J. S. and KUMP L. R. (1994) Lithologic and climatologic controls on river chemistry. *Geochim. Cosmochim. Acta* **58,** 2341–2359 (this issue).

BOHN H. L., MCNEAL B. L., and O'CONNOR G. A. (1979) *Soil Chemistry.* Wiley-Interscience.

BRADY P. V. (1991) The effect of silicate weathering on global temperature and atmospheric CO_2. *J. Geophys. Res.* **96,** 18101–18106.

BRADY P. V. (1992) Silicate surface chemistry at elevated temperatures. *Geochim. Cosmochim. Acta* **56,** 2941–2946.

BRADY P. V. and WALTHER J. V. (1989) Controls on silicate dissolution rates in neutral and basic pH solutions at 25 C. *Geochim. Cosmochim. Acta* **53,** 2823–2830.

BRADY P. V. and WALTHER J. V. (1990) Kinetics of quartz dissolution at low temperatures. *Chem. Geol.* **82,** 253–264.

BRADY P. V. and WALTHER J. V. (1992) Surface chemistry and silicate dissolution at elevated temperatures. *Amer. J. Sci.* **292,** 639–658.

BRANTLEY S. L., CRANE S. R., CRERAR D. A., HELLMANN R., and STALLARD R. (1986) Dissolution at dislocation etch pits in quartz. *Geochim. Cosmochim. Acta* **50,** 2349–2362.

BURCH T. E., NAGY K. L., and LASAGA A. C. (1994) Free energy dependence of albite dissolution kinetics at 80 C, pH 8.8. *Chem. Geol.* (in press).

BURTON W. K., CABRERA N., and FRANK F. C. (1951) The growth of crystals and the equilibrium structure of their surfaces. *Phil. Trans. Roy. Soc. London* **A243,** 299–358.

CARROLL S. A. (1989) The dissolution behavior of corundum, kaolinite, and andalusite: A surface complexation reaction model for the dissolution behavior of aluminosilicate minerals in diagenetic systems. Ph.D. dissertation, Northwestern Univ.

CARROLL S. A. and WALTHER J. V. (1990) Kaolinite dissolution at 25, 60 and 80°C. *Amer. J. Sci.* **290,** 797–810.

CARROLL-WEBB S. A. and WALTHER J. V. (1988) A surface complex reaction model for the pH-dependence of corundum and kaolinite dissolution rates. *Geochim. Cosmochim. Acta* **52,** 2609–2623.

CASEY W. H. and SPOSITO G. (1992) On the temperature dependence of mineral dissolution rates. *Geochim. Cosmochim. Acta* **56,** 3825–3830.

CASEY W. H., CARR M. J., and GRAHAM R. A. (1988) Crystal defects and the dissolution kinetics of rutile. *Geochim. Cosmochim. Acta* **52,** 1545–1556.

CASEY W. H., HOCHELLA M. F., and WESTRICH H. R. (1993) The surface chemistry of manganiferous silicate minerals as inferred from experiments on tephroite (Mn_2SiO_4). *Geochim. Cosmochim. Acta* **57,** 785–793.

CHOU L. and WOLLAST R. (1984) Study of the weathering of albite at room temperature and pressure with a fluidized bed reactor. *Geochim. Cosmochim. Acta* **48,** 2205–2217.

CHOU L. and WOLLAST R. (1985) Steady-state kinetics and dissolution mechanisms of albite. *Amer. J. Sci.* **285,** 963–993.

CORWIN J. F. and SWINNERTON A. C. (1951) The growth of quartz in alkali halide solutions. *J. Amer. Chem. Soc.* **73,** 3598–3602.

CYGAN R. T., CASEY W. H., BOSLOUGH M. B., WESTRICH H. R., CARR M. J., and HOLDREN G. R. (1989) Dissolution kinetics of experimentally shocked silicate minerals. *Chem. Geol.* **78,** 229–244.

DE GROOT S. R. and MAZUR P. (1962) *Nonequilibrium Thermodynamics.* North-Holland.

DOVE P. M. and CRERAR D. A. (1990) Kinetics of quartz dissolution in electrolytesolutions using a hydrothermal mixed flow reactor. *Geochim. Cosmochim. Acta* **54,** 955–969.

DOVE P. M. and ELSTON S. F. (1992) Dissolution kinetics of quartz in sodium chloride solutions: Analysis of existing data and a rate model for 25°C. *Geochim. Cosmochim. Acta* **56,** 4147–4156.

DREVER J. I. (1988) *The Geochemistry of Natural Waters* (2nd ed.). Prentice Hall.

FISHER G. W. and LASAGA A. C. (1981) Irreversible thermodynamics in petrology. In *Kinetics of Geochemical Processes* (ed. A. C. Lasaga and R. J. Kirkpatrick); *Rev. Mineral. 8,* pp. 171–209.

FURRER G. and STUMM W. (1986) The coordination chemistry of weathering: I Dissolution kinetics of σ-Al_2O_3 and BeO. *Geochim. Cosmochim. Acta* **50,** 1847–1860.

GAFFIN S. (1987) Ridge volume dependence on seafloor generation rate and inversion using long term sealevel change. *Amer. J. Sci.* **287,** 596–611.

GARRELS R. M. and CHRIST C. L. (1965) *Solutions, Minerals, and Equilibria.* Freeman, Cooper and Company.

GRANDSTAFF D. E. (1986) The dissolution rate of forsteritic olivine from Hawaiian beach sand. In *Rates of Chemical Weathering of Rocks and Minerals* (ed. S. M. Colman and D. P. Dethier), pp. 41–59. Academic.

HEINRICH W., METZ P., and BAYH W. (1986) Experimental investigation of the mechanism of the reaction: 1 tremolite + 11 dolomite = 8 forsterite + 13 calcite + 9 CO_2 + 1 H_2O. *Contrib. Mineral. Petrol.* **93,** 215–221.

HELGESON H. C. (1968) Evaluation of irreversible reactions in geochemical processes involving minerals and aqueous solutions-I. Thermodynamic relations. *Geochim. Cosmochim. Acta* **32,** 853–877.

HELGESON H. C. (1979) Mass transfer among minerals and hydrothermal solutions. In *Geochemistry of Hydrothermal Ore Deposits* (ed. H. L. Barnes), pp. 568–610. Wiley.

HELGESON H. C. and MURPHY W. M. (1983) Calculation of mass transfer among minerals and aqueous solutions as a function of time and surface area in geochemical processes. I. Computational Approach. *Math. Geol.* **15,** 109–130.

HELGESON H. C., MURPHY W. M., and AAGAARD P. (1984) Thermodynamic and kinetic constraints on reaction rates among minerals and aqueous solutions. II. Rate constants, effective surface area, and the hydrolysis of feldspar. *Geochim. Cosmochim. Acta* **48,** 2405–2432.

HOLDREN G. R. and SPEYER P. (1985) pH dependent changes in the rates and stoichiometry of dissolution of an alkali feldspar at room temperature. *Amer. J. Sci.* **285,** 994–1026.

HOLDREN G. R., CASEY W. H., WESTRICH H. R., and BOSLOUGH M. (1988) Bulk dislocation densities and dissolution rates in a calcic plagioclase. *Chem. Geol.* **70,** 79–85.

HOLLAND H. D. (1978) *The Chemistry of the Atmosphere and Oceans.* Wiley.

HOSAKA M. and TAKI S. (1981a) Hydrothermal growth of quartz crystals in NaCl solution. *J. Cryst. Growth* **52,** 837–842.

HOSAKA M. and TAKI S. (1981b) Hydrothermal growth of quartz crystals in NaCl solution. *J. Cryst. Growth* **53,** 542–546.

HUANG W. L. (1993) Stability and kinetics of kaolinite to boehmite conversion under hydrothermal conditions. *Chem. Geol.* **105,** 197–214.

KASTING J. F. (1984) Comments on the BLAG model: The carbonate-silicate geochemical cycle and its effect on atmospheric carbon dioxide over the past 100 million years. *Amer. J. Sci.* **284,** 1175–1182.

KINEMAN J. J. (1992) *Global Ecosystems Database.* EPA., Natl. Geophys. Data Ctr.

KLINE W. E. and FOGLER H. S. (1981a) Dissolution kinetics: Catalysis by strong acids. *J. Colloid Interface Sci.* **82,** 93–102.

KLINE W. E. and FOGLER H. S. (1981b) Dissolution kinetics: catalysis by salts. *J. Colloid Interface Sci.* **82,** 103–112.

KNAUSS K. G. and WOLERY T. J. (1986) Dependence of albite dissolution kinetics on pH and time at 25 C and 70 C. *Geochim. Cosmochim. Acta* **50,** 2481–2497.

KNAUSS K. G. and WOLERY T. J. (1988) The dissolution kinetics of quartz as a function of pH and time at 70 C. *Geochim. Cosmochim. Acta* **52,** 43–53.

KNAUSS K. G. and WOLERY T. J. (1989) Muscovite dissolution kinetics as a function of pH and time at 70 C. *Geochim. Cosmochim. Acta* **52,** 1493–1502.

LAIDLER K. J. (1987) *Chemical Kinetics.* Harper and Row.

LASAGA A. C. (1981a) Transition state theory, in A. C. Lasaga and R. J. Kirkpatrick, eds., Kinetics of Geochemical Processes. Rev. Mineral. 8, 135–169.

LASAGA A. C. (1981b) Rate laws in chemical reactions, In *Kinetics of Geochemical Processes* (ed. A. C. LASAGA and R. J. KIRKPATRICK); *Rev. Mineral. 8,* pp. 1–68.

LASAGA A. C. (1981c) The atomistic basis of kinetics: Defects in Minerals. In *Kinetics of Geochemical Processes* (ed. A. C. Lasaga and R. J. Kirkpatrick); *Rev. Mineral. 8,* pp. 261–319.

LASAGA A. C. (1983) Kinetics of silicate dissolution. In *Fourth Int. Symp. Water-Rock Interaction,* pp. 269–274. MIsasa.

LASAGA A. C. (1984) Chemical kinetics of water-rock interactions. *J. Geophys. Res.* **89,** 4009–4025.

LASAGA A. C. (1986) Metamorphic reaction rate laws and development of isograds. *Mineral. Mag.* **50,** 359–373.

LASAGA A. C. (1990) Atomic Treatment of Mineral-Water Surface Reactions. In *Mineral-Water Interface Geochemistry* (ed. M. F. Hochella and A. F. White); *Rev. Mineral. 23,* pp. 17–85.

LASAGA A. C. and BLUM A. E. (1986) Surface Chemistry, Etch Pits and Mineral-Water Reactions. *Geochim. Cosmochim. Acta* **50,** 2363–2379.

LASAGA A. C., BERNER R. A., and GARRELS R. M. (1985) An improved geochemical model of atmospheric CO_2 fluctuations over the past 100 million years. In *The Carbon Cycle and Atmospheric CO_2: Natural Variations Archean to Present* (ed. E. Sundquist and W. S. Broecker); *Geophys. Mono.* **32,** pp. 397–411.

LASAGA A. C. and GIBBS G. V. (1990) Ab-initio quantum mechanical calculations of water-rock interactions: Adsorption and hydrolysis reactions. *Amer. J. Sci.* **290,** 263–295.

LAUDISE R. A. (1958) Kinetics of hydrothermal quartz crystallization. *J. Amer. Chem. Soc.* **81,** 562–566.

LICHTNER P. C. (1985) Continuum model for simultaneous chemical reactions and mass transport in hydrothermal systems. *Geochim. Cosmochim. Acta* **49,** 779–800.

LICHTNER P. C. (1988) The quasi-stationary state approximation to coupled mass transport and fluid-rock interaction in a porous medium. *Geochim. Cosmochim. Acta* **52,** 143–165.

LIN F.-C. and CLEMENCY C. V. (1981) The kinetics of dissolution of muscovites at 25 C and 1 atm CO_2 partial pressure. *Geochim. Cosmochim. Acta* **52,** 143–165.

MACINNIS I. N. and BRANTLEY S. L. (1992) The role of dislocations and surface morphology in calcite dissolution. *Geochim. Cosmochim. Acta* **56,** 1113–1126.

MEYBECK M. (1979) Concentrations des eaux fluviales en elements majeurs et apports en solution aux oceans. *Rev. Geol. Dyn. Geogr. Phys.* **21,** 215–246.

MEYBECK M. (1980) Pathways of major elements from land to ocean through rivers: In *Proceedings of the review and workshop on river inputs to ocean-systems* (ed. J.-M. MARTIN et al.), pp. 18–30. FAO.

MEYBECK M. (1988) How to establish and use world budgets of riverine materials. In *Physical and Chemical Weathering in Geochemical Cycles* (ed. A. LERMAN and M. MEYBECK) pp. 247–272. Kluwer.

MOGOLLON J. L., GANOR J., SOLER J. M., and LASAGA A. C. (1994) Column experiments and the complex dissolution rate law of gibbsite. *Amer. J. Sci.* (in press).

MURPHY W. M. (1989a) Dislocations and feldspar dissolution. *Eur. J. Mineral.* **1,** 315–326.

MURPHY W. M. (1989b) Dislocations and feldspar dissolution: Theory and experimental data. *Chem. Geol.* **70,** 163–169.

MURR L. E. and HISKEY J. B. (1981) Kinetic effects of particle-size and crystal dislocation density on the dichromate leaching of chalcopyrite. *Metall. Trans.* **12B,** 255–267.

NAGY K. L. and LASAGA A. C. (1992) Dissolution and precipitation kinetics of gibbsite at 80 C and pH 3. The dependence on solution saturation state. *Geochim. Cosmochim. Acta* **56,** 3093–3111.

NAGY K. L. and LASAGA A. C. (1993) Simultaneous precipitation kinetics of kaolinite and gibbsite at 80°C and pH 3. *Geochim. Cosmochim. Acta* **57,** 4329–4335.

NAGY K. L., STEEFEL C. I., BLUM A. E., and LASAGA A. C. (1990) Dissolution and precipitation kinetics of kaolinite: Initial results at 80 C with application to porosity evolution in a sandstone. In *Prediction of Reservoir Quality through Chemical Modeling* (ed. I. D. Meshri and P. J. Ortoleva); *Amer. Assoc. Petrol. Geol. Mem. 49,* pp. 85–101.

NAGY K. L., BLUM A. E., and LASAGA A. C. (1991) Dissolution and precipitation kinetics of kaolinite at 80 C and pH 3. The dependence on solution saturation state. *Amer. J. Sci.* **291,** 649–686.

NAHON D. B. (1991) *Introduction to the Petrology of Soils and Chemical Weathering.* Wiley-Interscience.

NIELSEN A. E. (1984) Electrolyte crystal growth mechanisms. *J. Cryst. Growth* **67,** 289–310.

NIELSEN A. E. (1986) Mechanisms and rate laws in electrolyte crystal growth from aqueous solution. In *Geochemical Processes at Mineral Surfaces* (ed. J. A. DAVIS and K. F. HAYES) *ACS Symp. Ser. 323.* Chap. 29.

NIELSEN A. E. and TOFT J. M. (1984) Electrolyte crystal growth kinetics. *J Cryst. Growth* **67,** 278–288.

OHARA M. and REID R. C. (1973) *Modeling Crystal Growth Rates from Solution.* Prentice-Hall.

PITCHER E. J., MALONE R. C., RAMANATHAN V., BLACKMON M. L., PURI K., and BOUORKE W. (1983) January and July simulations with a spectral general circulation model. *J. Atmos. Sci.* **40,** 580–604.

RAMANATHAN V., PITCHER E. J., MALONE R. C., and BLACKMON M. L. (1983) The response of a spectral general circulation model to refinements in radiative processes. *J. Atmos. Sci.* **40,** 605–631.

RAYMO M. E. and RUDDIMAN W. F. (1992) Tectonic forcing of late Cenozoic climate. *Nature* **359,** 117–122.

RIMSTIDT J. D. and BARNES H. L. (1980) The kinetics of silica-water reactions. *Geochim. Cosmochim. Acta* **44,** 1683–1700.

RIMSTIDT J. D. and DOVE P. M. (1986) Mineral/solution reaction rates in a mixed flow reactor: Wollastonite hydrolysis. *Geochim. Cosmochim. Acta* **50,** 2509–2516.

RONOV A. B. (1976) Global carbon geochemistry, volcanism, carbonate accumulation, and life. *Geochem. Intl.* **13,** 172–195.

ROSE N. M. (1991) Dissolution rates of prehnite, epidote, and albite. *Geochim. Cosmochim. Acta* **55,** 3273–3286.

SCHOTT J., BRANTLEY S., CRERAR D., GUY C., BORCSIK M., and WILLAIME C. (1989) Dissolution kinetics of strained calcite. *Geochim. Cosmochim. Acta* **53,** 373–382.

SCHRAMKE J. A., KERRICK D. M., and LASAGA A. C. (1987) The reaction muscovite + quartz = andalusite + K-feldspar + water. Part I. Growth kinetics and mechanism. *Amer. J. Sci.* **287,** 517–559.

SCHWEDA P. S. (1989) Kinetics of alkali feldspar dissolution at low temperature. In *Water-Rock Interaction,* pp. 609–612. Balkema.

STALLARD R. F. (1988) Weathering and erosion in the humid tropics. In *Physical and Chemical Weathering in Geochemical Cycles* (ed. A. LERMAN and M. MEYBECK), pp. 225–246. Kluwer.

STALLARD R. F. and EDMOND J. M. (1983) Geochemistry of the Amazon. 2: The influence of geology and weathering environment on the dissolved load. *J. Geophys. Res.* **88,** 9671–9688.

STEEFEL C. I. and LASAGA A. C. (1990) The evolution of dissolution patterns: permeability change due to coupled flow and reaction, In *Chemical Modeling of Aqueous Systems II* (ed. D. C. MELCHIOR and R. L. BASSETT); *Amer. Chem. Soc. Symp. Ser. 416,* pp. 212–225.

STEEFEL C. I. and LASAGA A. C. (1992) Putting transport into water-rock interaction models. *Geology* **20,** 680–684.

STEEFEL C. I. and LASAGA A. C. (1994) A coupled model for transport of multiple chemical species and kinetic precipitation/dissolution reactions with application to reactive flow in single phase hydrothermal systems. *Amer. J. Sci.* **294,** 529–592.

STEEFEL C. I. and VAN CAPPELLEN P. (1990) A new approach to modeling water-rock interaction: the role of precursors, nucleation, and Ostwald ripening. *Geochim. Cosmochim. Acta* **54,** 2657–2677.

STUMM W. and WIELAND E. (1990) Dissolution of oxide and silicate minerals: Rates depend on surface speciation. In *Aquatic Chemical Kinetics* (ed. W. STUMM), pp. 367–400. Wiley.

STUMM W. and WOLLAST R. (1990) Coordination chemistry of weathering: Kinetics of surface-controlled dissolution of oxide minerals. *Rev. Geophys.* **28,** 53–69.

STUMM W., FURRER G., and KUNZL B. (1983) The role of surface coordination in precipitation and dissolution of mineral phases. *Croat. Chem. Acta* **56,** 593–611.

STUMM W., FURRER G., WIELAND E., and ZINDER B. (1985) The effects of complex-forming ligands on the dissolution of oxides and aluminosilicates. In *The Chemistry of Weathering* (ed. J. I. DREVER), pp. 55–74. Reidel.

TARDY Y. (1969) Geochimie des alterations. Étude des arènes et des eaux de quelques massifs cristallins d'Europe et d'Afrique. *Mem. Serv. Carte Geol.*

TOLE M. P. (1987) Thermodynamic and kinetic aspects of formation of bauxites. *Chem. Geol.* **60,** 95–100.

TOLE M. P., LASAGA A. C., PANTANO C., and WHITE W. B. (1986) The kinetics of dissolution of nepheline ($NaAlSiO_4$). *Geochim. Cosmochim. Acta* **50,** 379–392.

VELBEL M. A. (1985) Geochemical mass balances and weathering rates in forested watersheds of the southern Blue Ridge. *Amer. J. Sci.* **285,** 904–930.

VOLK T. (1987) Feedbacks between weathering and atmospheric CO_2 over the last 100 million years. *Amer. J. Sci.* **287,** 763–779.

WIELAND E., WEHRLI B., and STUMM W. (1988) The coordination chemistry of weathering: III. A generalization on the dissolution rates of minerals. *Geochim. Cosmochim. Acta* **52,** 1969–1981.

WILLIAMSON D. L., KIEHL J. T., RAMANATHAN V., DICKINSON R. E., and HACK J. J. (1987) Description of NCAR community climate model (CCM1). *NCAR Tech. Note NCAR/TN-285 + STR,* pp. 112.

WOGELIUS R. A. and WALTHER J. V. (1991) Olivine dissolution at 25°C: Effects of pH, CO_2 and organic acids. *Geochim. Cosmochim. Acta* **55,** 943–954.

XIE Z. and WALTHER J. V. (1992) Incongruent dissolution and surface area of kaolinite. *Geochim. Cosmochim. Acta* **56,** 3357–3363.